Global and Planetary Change 167 (2018) 172–189

Contents lists available at ScienceDirect

Global and Planetary Change

journal homepage: www.elsevier.com/locate/gloplacha

Review article

Clumped isotope record of salinity variations in the Subboreal Province at the Middle–Late Jurassic transition

Hubert Wierzbowski[a,*], David Bajnai[b], Ulrike Wacker[b,c], Mikhail A. Rogov[d], Jens Fiebig[b], Ekaterina M. Tesakova[d,e]

[a] Polish Geological Institute – National Research Institute, Rakowiecka 4, Warsaw 00-975, Poland
[b] Institute of Earth Sciences, J.W. Goethe University, Altenhöferallee 1, Frankfurt 60487, Germany
[c] Thermo Fisher Scientific, Hanna-Kunath-Straße 11, Bremen 28199, Germany
[d] Geological Institute, Russian Academy of Sciences, Pyzhevsky lane 7, Moscow 119017, Russia
[e] Faculty of Geology, M.V. Lomonosov Moscow State University, Leninskie Gory, Moscow 119234, Russia

ARTICLE INFO

Keywords:
Middle Russian Sea
Stable isotopes
Elemental ratios
Belemnite rostra
Ammonite shells
Palaeoceanography

ABSTRACT

Results of clumped isotope, oxygen isotope and elemental (Mg/Ca, Sr/Ca) analyses of exceptionally well-preserved belemnite rostra and ammonite shells from the uppermost Callovian–Upper Kimmeridgian (Lamberti–Mutabilis zones) of the Russian Platform are presented. Despite a significant decrease in belemnite $\delta^{18}O$ values across the Upper Oxfordian–Lower Kimmeridgian, the clumped isotope data show a constant seawater temperature (ca. 16 °C) in the studied interval. The decrease in belemnite $\delta^{18}O$ values and lower $\delta^{18}O$ values measured from ammonite shells are interpreted as a result of the salinity decline of the Middle Russian Sea of ca. 12‰, and salinity stratification of the water column, respectively. The postulated secular palaeoenvironmental changes are linked to the inflow of subtropical, saline waters from the Tethys Ocean during a sea-level highstand at the Middle–Late Jurassic transition, and progressive isolation and freshening of the Middle Russian Sea during the Late Oxfordian–Kimmeridgian.

The obtained clumped isotope data demonstrate relative stability of the Late Jurassic climate and a paramount effect of local palaeoceanographic conditions on carbonate $\delta^{18}O$ record of shallow epeiric seas belonging to the Subboreal Province. Variations in Mg/Ca and Sr/Ca ratios of cylindroteuthid belemnite rostra, which are regarded by some authors as temperature proxies, are, in turn, interpreted to be primarily dependent on global changes in seawater chemistry.

The paleoenvironmental variations deduced from clumped and oxygen isotope records of the Russian Platform correspond well with changes in local cephalopod and microfossil faunas, which show increasing provincialism during the Late Oxfordian and the Early Kimmeridgian. Based on the review of literature data it is suggested that the observed salinity decrease and restriction of Subboreal basins during the Late Jurassic played a major role in the formation of periodic bottom water anoxia and sedimentation of organic rich facies.

1. Introduction

A short-term global climate cooling at the Middle–Late Jurassic transition (Late Callovian–Middle Oxfordian) or the incursion of cold Boreal waters are inferred from oxygen isotope records of marine calcareous shells and tooth phosphates of Western and Central Europe, and the Russian Platform (Dromart et al., 2003; Lécuyer et al., 2003; Nunn et al., 2009; Price and Rogov, 2009; Wierzbowski et al., 2009; Wierzbowski and Rogov, 2011; Wierzbowski et al., 2013; Wierzbowski, 2015). A subsequent Late Oxfordian–Early Kimmeridgian warming is suggested for various palaeogeographical areas (Abbink et al., 2001; Brigaud et al., 2008; Nunn et al., 2009; Žak et al., 2011; Alberti et al., 2012a, 2012b; Jenkyns et al., 2012; Wierzbowski et al., 2013; Wierzbowski, 2015). The oxygen isotope record of restricted European marine basins being a primary proxy for palaeoclimate reconstructions may, however, be affected by local salinity variations linked to changes in the water circulation and the palaeobathymetry. Although the Late Oxfordian–Early Kimmeridgian warming is regarded as a supra-regional, common phenomenon (cf. Dromart et al., 2003; Lécuyer et al., 2003; Brigaud et al., 2008; Nunn et al., 2009; Žak et al., 2011; Alberti

* Corresponding author.
E-mail addresses: hubert.wierzbowski@pgi.gov.pl (H. Wierzbowski), david.bajnai@em.uni-frankfurt.de (D. Bajnai), ulrike.wacker@thermofisher.com (U. Wacker), jens.fiebig@em.uni-frankfurt.de (J. Fiebig).

https://doi.org/10.1016/j.gloplacha.2018.05.014
Received 19 January 2018; Received in revised form 29 May 2018; Accepted 29 May 2018
Available online 06 June 2018

et al., 2012a, 2012b; Wierzbowski et al., 2013; Arabas, 2016) its magnitude in marginal marine basins seems to be overestimated due the effect of increasing freshwater runoff under a global sealevel fall (cf. Wierzbowski et al., 2013; Wierzbowski, 2015). A particular case is the oxygen isotope record of belemnite rostra from the Russian Platform showing a dramatic decrease in $\delta^{18}O$ values of ca. 3‰ throughout the Oxfordian–Kimmeridgian (cf. Riboulleau et al., 1998; Dromart et al., 2003; Price and Rogov, 2009), which may be only partially attributed to a temperature rise (Wierzbowski et al., 2013).

The clumped isotope composition of well-preserved calcium carbonate minerals is an independent proxy for precipitation temperatures. Determination of both the clumped and the oxygen isotopic compositions of carbonates allows reconstruction of ancient $\delta^{18}O_{water}$ values (Ghosh et al., 2006; Eiler, 2011). Clumped isotope analyses have been successfully used for the reconstruction of water temperatures during the growth of carbonate fossils (cf. Finnegan et al., 2011; Dennis et al., 2013; Price and Passey, 2013; Tobin et al., 2014; Petersen et al., 2016).

The aim of the study is to determine real variations of water temperature of the Middle Russian Sea belonging to the Subboreal bioprovince during and after the Middle–Late Jurassic transition (the latest Callovian–earliest Late Kimmeridgian). For this exceptionally well-preserved belemnite rostra and ammonite shells from the Volga Basin in the European part of Russia were analysed. The comparison between carbonate Δ_{47} and $\delta^{18}O$ values allow determination of ancient water $\delta^{18}O$ values, which may be linked to salinity fluctuations of the restricted Middle Russian Sea. The isotope data and their interpretation are compared with the distribution of macro- and microfossils in the Russian Platform to verify palaeoenvironmental reconstructions. The present study sheds new light on the latest Middle Jurassic–Late Jurassic climate and effects of local palaeobathymetry and palaeocirculation on climate reconstructions based on $\delta^{18}O$ values of marine fossils derived from epicontinental or marginal sea basins.

2. Material

Well-preserved and stratigraphically well-dated 19 archival and 5 newly collected belemnite rostra and ammonite shells have been analysed for their clumped isotope composition in order to obtain a continuous record of temperature variations of the epicontinental Middle Russian Sea during and after the Middle–Late Jurassic transition (the latest Callovian–mid-Kimmeridgian; see Table 1). The archival uppermost Callovian–Lower Kimmeridgian materials (cylindroteuthid and mesohibolitid belemnite rostra and ammonite shells) derived from the Dubki section near Saratov, and the Makar'ev and Mikhalenino sections in the Kostroma Region of Russia (Fig. 1) comprise samples studied by Wierzbowski and Rogov (2011), and Wierzbowski et al. (2013). The newly collected cylindroteuthid rostra, studied for clumped isotopes, are derived from Tarkhanovskaya Pristan' section near Ul'yanovsk in the Tatarstan Republic of the Russian Federation (Fig. 1). They are dated to the latest Early Kimmeridgian–earliest Late Kimmeridgian, i.e., the late Cymodoce Zone (= Divisum Zone) and the Mutabilis Zone (cf. Rogov et al., 2017, and Table 1). Some of these samples have been studied recently for strontium isotope composition (Wierzbowski et al., 2017). In addition, results of new oxygen and carbon isotope analyses of 19 Kimmeridgian cylindroteuthid belemnite rostra and 175 published values of carbonate fossils (cylindroteuthid and mesohibolitid belemnite rostra, ammonite and gastropod shell; see Wierzbowski and Rogov, 2011; Wierzbowski et al., 2013) are presented.

Collected carbonate fossils are precisely biostratigraphically dated (see Wierzbowski and Rogov, 2011; Wierzbowski et al., 2013; Table 1). The standard Boreal and the Subboreal ammonite zonal schemes are employed for dating of uppermost Callovian–Oxfordian and Kimmeridgian sediments, respectively, according to the regional biostratigraphical framework (Fig. 2). It is worth noting that occurrences of Submediterranean ammonites allow the use of Submediterranean biostratigraphical units in some parts of the studied sections (Głowniak et al., 2010; Rogov et al., 2017). Precise correlation between the (Sub) Boreal ammonite zonal scheme of the Oxfordian–lowermost Upper Kimmeridgian of the Russian Platform and the Submediterranean province of central Europe zonation is presented on Fig. 2. The employed biostratigraphical scale is matched to the assumed equal duration of Submediterranean ammonites subchrons, which are counted successively starting from the base of the studied interval (cf. Wierzbowski et al., 2013). This approach is used to enable direct comparison between the recorded isotope variations and the previously published isotope data from Western and Central Europe.

3. Methodology

3.1. Preparation

Thin sections prepared from newly collected belemnite rostra were studied by means of an optical microscope coupled with a CCL Mk5–2 Cambridge Image Technology Ltd. cold cathode device. The rostra were cleaned, using a hand-held drill, from adherent sediment, apical-line areas, alveolar fissure infillings and, if necessary, narrow luminescent rims or veins. Fragments of the studied belemnite rostra comprising most growth rings, and derived from *rostrum solidum* (cf. Sælen, 1989) were powdered and homogenised in an agate mortar. Each specimen yielded 100–300 mg of carbonate powder. Aliquots of the same carbonate powders were used for chemical, oxygen, carbon and clumped isotope analyses. For clumped isotope analyses aliquots of carbonate samples studied previously by Wierzbowski and Rogov (2011), and Wierzbowski et al. (2013) were also used. The archival samples had been prepared and screened for the state of preservation in the same way (cf. Wierzbowski and Rogov, 2011; Wierzbowski et al., 2013).

3.2. Chemical analyses

Ca, Mg, Mn, Fe, Sr and Na concentrations were determined by the ICP-OES (Inductively Coupled Plasma Optical Emission Spectrometry) method using Thermo iCAP 6500 Duo system at the Polish Geological Institute–National Research Institute in Warsaw (Poland). 50–100 mg aliquots of the carbonate powders were dissolved in 5 wt% hydrochloric acid. Reproducibility of chemical analyses (2σ S.D.) was controlled by multiple analyses of measured samples and averages as follows: 1.0% for Ca, 2.4% for Mg, 2.2% for Sr, 0.8% for Mn, 2.7% for Fe, and 1.4% for Na. Repeated analyses of JLs-1 calcite and JDo-1 dolomite references (cf. Imai et al., 1996) yielded accuracies of measurements (2σ S.D.) better than 3.5% for Ca, 3.8% for Mg, 1.0% for Sr, and 4.0% for Mn. The accuracy of Fe analyses cannot be given precisely due to the employed dissolution method in weak hydrochloric acid, which is not relevant for the determination of non-carbonate iron compounds present in the both standards. In addition, Na contents of the both references are much lower than those of studied belemnite samples, therefore, the accuracy of measurements of Na concentrations cannot be precisely verified.

3.3. Clumped isotope analyses

The clumped isotope analyses were conducted between April 2015 and July 2017 at the Institute of Earth Sciences, Goethe University, Frankfurt, Germany, following the procedure described in Bajnai et al. (2018). Clumped isotope composition of all samples was measured in at least five replicates. Carbonate digestion and CO_2 purification were made on a fully automated preparation line. For each replicate analysis, ca. 6 mg of homogenised carbonate powder was reacted at 90 °C, for 30 min, with > 105% phosphoric acid. The resultant CO_2 was purified cryogenically five times using a Porapak Q trap cooled down to −15 °C. The sample gas was measured alternately with a reference gas of known isotopic composition using the dual-inlet system of a ThermoFisher

Table 1
Stratigraphy, chemical and isotope data of analysed samples from the Russian Platform.

Sample	Locality	(Sub)zone	Position	Taxonomy	Ca wt%	Mg ppm	Mg/Ca *1000	Sr ppm	Sr/Ca *1000	Mn ppm	Fe ppm	Na ppm	$\delta^{13}C$ ‰	$\delta^{18}O$ ‰	Δ_{47} ‰	Δ_{47} error 1 S.E.	T °C	T_{error} 1 S.E.
RT2a	Tarkh. Pr	Orthocera/ Lallieranum	28.50	*Pachyteuthis (Boreioteuthis) aff, troslayana (?)*	38.7	1162	4.95	1290	1.52	1	< 20	1124	2.20	−1.12	–	–	–	–
RT1b[C]	Tarkh. Pr.	Lallieranum	28.26	*Lagonibelus kostromensis* (?)	38.7	2024	8.62	1253	1.48	2	< 20	1482	0.36	−1.57	–	–	–	–
RT1a[C]	Tarkh. Pr.	Lallieranum	28.26	*Cylindroteuthis* sp. (?)	38.7	1585	6.75	1276	1.51	2	< 20	1281	1.14	−1.32	–	–	–	–
RT15[C]	Tarkh. Pr.	Lallieranum	27.81	*Cylindroteuthis cuspidata*	38.5	1463	6.27	1269	1.51	4	< 20	1194	0.38	−1.55	0.702	0.007	13.2	2.6
RT24b	Tarkh. Pr.	Lallieranum	27.62	*Cylindroteuthis* sp.	38.9	1770	7.50	1040	1.22	< 1	< 20	1258	1.01	−0.99	–	–	–	–
RT24a[C]	Tarkh. Pr.	Lallieranum	27.62	*Cylindroteuthis cuspidata*	38.2	1591	6.87	1102	1.32	2	< 20	1220	1.33	−1.40	–	–	–	–
RT16[C]	Tarkh. Pr.	Mutabilis	26.62	*Cylindroteuthis cuspidata*	38.3	1357	5.84	1235	1.47	1	< 20	1180	1.28	−1.36	0.689	0.008	17.9	2.9
RT20[C]	Tarkh. Pr.	Askepta	25.78	indeterminable	38.7	1322	5.63	1143	1.35	2	< 20	1141	2.28	−1.71	0.699	0.003	14.3	1.1
RT6	Tarkh. Pr.	Askepta	25.68	*Cylindroteuthis* cf. *cuspidata*	38.9	1346	5.71	1197	1.41	3	< 20	1098	2.55	−1.53	–	–	–	–
RT17	Tarkh. Pr.	Askepta	25.56	*Cylindroteuthis cuspidata*	38.4	1684	7.23	1171	1,39	4	< 20	1363	1.32	−1.30	0.688	0.005	18.1	1.7
RT10	Tarkh. Pr.	Askepta	25.56	indeterminable	38.3	1751	7.54	1253	1.50	7	< 20	1290	2.14	−1.33	0.690	0.006	17.7	2.2
RT3	Tarkh. Pr.	Askepta	25.56	*Cylindroteuthis cuspidata*	39.9	1569	6.48	1247	1.43	2	< 20	1329	1.51	−1.91	–	–	–	–
RT4[C]	Tarkh. Pr.	Askepta	25.54	*Cylindroteuthis* cf. *cuspidata*	39.0	1292	5.46	1235	1.45	2	< 20	1254	2.38	−1.15	–	–	–	–
RT13	Tarkh. Pr.	Askepta	25.54	*Cylindroteuthis* sp.	38.7	1639	6.98	1131	1.34	5	< 20	1095	2.17	−1.54	–	–	–	–
RT23	Tarkh. Pr.	Askepta	25.52	*Cylindroteuthis cuspidata*	39.0	1302	5.50	1192	1.40	2	33	1100	2.06	−1.15	–	–	–	–
RT14	Tarkh. Pr.	Askepta	25.52	indeterminable	38.1	1629	7.05	1213	1.46	3	< 20	1227	1.20	−1.59	–	–	–	–
RT21[C]	Tarkh. Pr.	Askepta	25.46	*Cylindroteuthis cuspidata*	38.6	1594	6.81	1144	1.36	6	< 20	1265	1.65	−1.13	–	–	–	–
RT8[C]	Tarkh. Pr.	Askepta	25.40	*Cylindroteuthis cuspidata*	38.1	1813	7.85	1192	1.43	9	< 20	1270	0.72	−1.74	–	–	–	–
RT11	Tarkh. Pr.	Askepta	24.80	*Cylindroteuthis* cf. *cuspidata*	38.4	1392	5.98	1099	1.31	20	20	1262	1.59	−1.65	–	–	–	–
RMII43[B]	Mikhalen.	Cymodoce	19.99	*Pachyteuthis (P.) panderiana sp. nov. aff. P. sarygulensis*	37.6	1670	7.32	1160	1.41	4	< 20	1255	2.54	−0.76	0.701	0.008	13.7	2.9
RM98a[B]	Mikhalen.	Normand.	19.50	*Pachyteuthis* sp.	39.0	1401	5.92	1230	1.44	2	< 20	1110	2.88	−1.08	0.692	0.005	16.8	2.0
RMII42[B]	Mikhalen.	Normand.	19.49	*Pachyteuthis* cf. *(P.)excentralis*	37.8	1893	8.26	1291	1.56	2	< 20	1487	2.72	−0.93	0.700	0.005	13.7	1.7
RM15[B]	Mikhalen.	Rosenkrant.	14.08	*Pachyteuthis (P.) excentralis*	38.7	1435	6.11	1080	1.28	2	< 20	1269	2.28	0.10	0.694	0.006	16.0	2.3
RM1[B]	Mikhalen.	Regulare	13.79	*Pachyteuthis (Boreioteuthis) absoluta*	38.5	1360	5.82	1046	1.24	2	< 20	1250	2.93	0.24	0.678	0.004	22.3	1.8
RM100b[B]	Mikhalen.	Regulare	13.63	*Pachyteuthis* sp.	38.0	1203	5.22	1023	1.23	2	< 20	1195	2.25	0.40	0.693	0.005	16.3	1.7
RMII92[B]	Makar'ev	Vertebrale	8.10	*Pachyteuthis* sp.	37.6	1366	5.99	834	1.01	9	< 20	1053	1.42	1.63	0.711	0.004	10.0	1.5
RMII52a[B]	Makar'ev	Vertebrale	7.58	*Pachyteuthis (P.) panderiana*	38.0	967	4.20	878	1.06	1	< 20	1087	3.31	1.66	0.701	0.006	13.6	2.3
RMII50[B]	Makar'ev	Vertebrale	7.58	ammonite	aragonite ≥ 99%	–	–	–	–	–	–	–	2.29	−1.78	0.699	0.003	14.3	1.1
RMII103b[B]	Makar'ev	Vertebrale	6.98	ammonite	aragonite ≥ 99%	–	–	–	–	–	–	–	3.45	−1.48	0.716	0.011	8.3	3.6
RMII63[B]	Makar'ev	Vertebrale	6.60	*Pachyteuthis (P.) miatschkoviensis*	38.1	1080	4.67	824	0.99	2	< 20	1038	2.81	1.61	0.681	0.008	21.1	3.1
R96[A]	Dubki	Praecordat.	2.70	*Hibolithes* sp.	38.6	3936	16.80	1201	1.42	6	1	–	2.32	0.96	0.692	0.006	16.9	2.3
R124[A]	Dubki	Praecordat.	2.60	*Cylindroteuthis* sp.	39.1	1231	5.19	849	0.99	2	5	–	1.86	1.62	0.694	0.007	16.2	2.8
R134a[A]	Dubki	Praecordat.	2.48	*Cylindroteuthis* sp.	39.7	1197	4.97	972	1.12	4	17	–	2.95	1.63	0.687	0.008	18.7	3.0
R48/1[A]	Dubki	Scarburgen.	1.69	ammonite (*Cardioceras* sp.?)	aragonite ≥ 99%	–	–	–	–	–	–	–	2.70	1.20	0.700	0.007	13.9	2.4
R137a[A]	Dubki	Scarburgen.	1.25	*Hibolithes* sp.	38.1	4707	20.36	1230	1.48	4	6	–	2.06	0.89	0.685	0.005	19.5	1.8
R37[A]	Dubki	Lamberti	0.97	*Cylindroteuthis* sp.	39.0	1568	6.63	869	1.02	2	4	–	1.82	1.71	0.688	0.006	18.3	2.2
R150[A]	Dubki	Lamberti	0.79	*Cylindroteuthis* sp.	39.3	1023	4.30	928	1.08	1	7	–	2.59	1.97	0.697	0.006	14.8	2.4
R111/1[A]	Dubki	Lamberti	0.72	ammonite (*Sublunuloceras* sp.)	aragonite ≥ 99%	–	–	–	–	–	–		2.27	0.31	0.701	0.008	13.3	2.9

[A] Samples whose elemental concentrations and δ values are reported after Wierzbowski and Rogov (2011).
[B] Samples whose elemental concentrations and δ values are reported after Wierzbowski et al. (2013).
[C] Samples, whose elemental concentrations are reported after Wierzbowski et al. (2017).

Fig. 1. Location of studied outcrops on the Russian Platform. Mak. – Makar'ev, Mal. – Mal'gino, Mikh. – Mikhalenino, Tar. Pr. – Tarkhanovskaya Pristan', Yak. – Yakimikha,.

MAT 253 gas-source isotope-ratio mass spectrometer. For measurements carried out before May 2016 an Oztech reference gas ($\delta^{18}O$ = 25.01‰ VSMOW; $\delta^{13}C$ = −3.63‰ VPDB) was used and from May 2016 onwards an Alphagas Izotop reference gas ($\delta^{18}O$ = 25.56‰ VSMOW; $\delta^{13}C$ = −4.30‰ VPDB) was utilized. Background correction was performed for the sample and the reference gas separately, according to the procedure described by Fiebig et al. (2016).

Raw Δ_{47} values were calculated using the [*Gonfiantini/Santrock*] set of isotopic parameters (R^{13}_{PDB} = 0.0112372, R^{18}_{VSMOW} = 0.0020052, R^{17}_{VSMOW} = 0.0003799, λ = 0.5164). The values were projected to the CDES (Carbon Dioxide Equilibrium Scale) using equilibrated gases (Dennis et al., 2011). Empirical transfer functions (ETFs) were determined using gases of various bulk isotopic compositions equilibrated at 25 °C and 1000 °C (Supplementary Data 1). A 25 °C–90 °C acid fractionation factor of 0.069‰ (Guo et al., 2009) was applied to all $\Delta_{47\ (CDES\ 25)}$ values.

Seven carbonate standards were analysed along with the samples to confirm the precision and reproducibility of the measurements. The mean $\Delta_{47\ (CDES\ 25)}$ values (± 1σ S.D.) of the reference materials, for the whole period of measurements, are: Carrara (marble, calcite, *n* = 278) 0.389(± 0.020)‰, MuStd (*Arctica islandica*, aragonite, *n* = 166) 0.732(± 0.018)‰, Strauss (ostrich egg, calcite, n = 27) 0.656(± 0.029)‰, ETH-1 (calcite, *n* = 32) 0.283(± 0.015)‰, ETH-2 (calcite, *n* = 9) 0.280(± 0.023)‰, ETH-3 (calcite, *n* = 38) 0.700(± 0.020)‰, ETH-4 (calcite, *n* = 7) 0.556(± 0.033)‰ (Supplementary Data 1). These values are indistinguishable within ≤0.010% from corresponding $\Delta_{47\ (CDES\ 25)}$ values obtained elsewhere (Wacker et al., 2014, 2016; Fiebig et al., 2016; Bajnai et al., 2018).

$\Delta_{47\ (CDES\ 25)}$–temperature calibration of Wacker et al. (2014) was used to convert the measured clumped isotope values to precipitation temperatures of calcium carbonate (Eq. (1)).

$$\Delta_{47\,(CDES\,25)} = 0.0327^{*}\,10^{6}/T^{2} + 0.3030 \quad (1)$$

where T is the temperature in Kelvin. This calibration is based on calcium carbonate of various origin and was made at the Institute of Earth Sciences, Goethe University, Frankfurt, using the same analytical setup as in the present study. Wacker et al.'s (2014) calibration is identical to empirical calibration based on molluscs of Henkes et al. (2013). The steeper sloped calibration of Bonifacie et al. (2017) gives temperatures indistinguishable within ± 1σ S.E. from those calculated using Wacker et al.'s (2014) equation (see Supplementary Data 1). Previous studies have shown that the Δ_{47}–temperature relationships for calcite and aragonite are indistinguishable from each other (Tripati et al., 2010; Henkes et al., 2013; Defliese et al., 2015), allowing the use of the same calibration for both calcium carbonate mineralogies.

3.4. Oxygen and carbon isotope analyses

Oxygen and carbon isotope analyses of newly collected mid-Kimmeridgian belemnite rostra have been performed at the GeoZentrum Nordbayern, University of Erlangen-Nuremberg, Erlangen, Germany. Samples were reacted with 100% phosphoric acid at 70 °C using a Gasbench II connected to a ThermoFisher Delta V Plus mass spectrometer. All values are reported in per mil relative to VPDB scale by assigning a $\delta^{13}C$ and $\delta^{18}O$ value of +1.95‰ and − 2.20‰ to NBS19 and − 46.6‰ and − 26.7‰ to LSVEC, respectively. The reproducibility and accuracy of the measurements was monitored, over the course of analyses, by replicate analysis of laboratory standards Sol 2 (n = 10) and Erl 5 (n = 8). Reproducibility for $\delta^{13}C$ and $\delta^{18}O$ values was 0.04‰ and 0.03‰ (± 1σ S.D.) for Sol 2, and 0.06‰ and 0.05‰ (± 1σ S.D.) for Erl 5, respectively.

To calculate $\delta^{18}O$-derived temperatures and water $\delta^{18}O$ values for calcite a relationship of O'Neil et al. (1969) modified by Friedman and O'Neil (1977), Eq. (2) along with the SMOW to PDB scales conversion given by Friedman and O'Neil (1977), was used.

$$1000\ln\alpha_{calcite-water} = 2.\ 78^{*}10^{6}/T^{2}-2.89 \quad (2)$$

where $\alpha_{calcite-water}$ is the oxygen isotope fractionation factor between calcite and water, and T is the temperature in Kelvin.

To calculate $\delta^{18}O$-derived temperatures and water $\delta^{18}O$ values for aragonite a relationship established by Böhm et al. (2000), Eq. (3), along with the VSMOW to VPDB scales conversion given by Coplen et al. (1983), was used.

$$1000\ln\alpha_{aragonite-water} = 18.\ 45^{*}10^{3}/T-32.54 \quad (3)$$

where $\alpha_{aragonite-water}$ is the oxygen isotope fractionation factor between aragonite and water and T is the temperature in Kelvin. Since the $1000\ln\alpha_{aragonite-water}$ temperature relationship of Böhm et al. (2000) is based on $\delta^{18}O$ values of aragonite samples assigned directly to a calcite reference NBS 19, and measured at similar laboratory conditions as our samples, in the present study we report $\delta^{18}O$ values of aragonite ammonite and gastropod samples referenced to calcite standards (Table 1). The reported values differ slightly from those published previously by Wierzbowski and Rogov (2011), and Wierzbowski et al. (2013), which were re-calculated using a temperature-specific CO_2-acid fractionation factor for aragonite.

4. Results

4.1. Diagenetic alteration

The stable isotope composition of carbonates is susceptible to alteration in burial and meteoric environments. Diagenetic alteration of marine calcites often leads to significant enrichments in manganese and iron or to strontium depletion (Veizer, 1974, 1983; Brand and Veizer, 1980; Marshall, 1992; Ullmann and Korte, 2015). The chemical

SUBMEDITERRANEAN PROVINCE				(SUB)BOREAL PROVINCE			
Substage	Zone	Subzone	Position of the base	Position of the base	Subzone	Zone	Substage
Up. Kimmeridgian (pars)	Acanthicum		26.5	27.5	Lallieranum	Mutabilis	Up. Kimmeridgian (pars)
				26.5	Mutabilis		
Lower Kimmeridgian	Divisum	Uhlandi	25.5	24.25	Askepta	Cymodoce	Lower Kimmeridgian
		Tenuicostata	24.5				
	Hypselocyclum	Lothari	23.5	19.77	Cymodoce		
		Hyppolytense	22.5				
	Platynota	Guilherandense	21.5				
		Desmoides	20.5				
		Polygyratus	19.5				
"Former uppermost Oxfordian"	Planula	Galar	18.5	17.24	Normandiana	Baylei	
		Planula	17				
	Bimammatum	Hauffianum	16	15	Densicostata		
		Bimammatum	15				
Upper Oxfordian	Hypselum		14	14		Rosenkrantzi	Upper Oxfordian
	Bifurcatus	Grossouvrei	13	13.1		Regulare	
		Stenocycloides	12	12.73	Serratum	Serratum	
		Wartae	11	12.33	Koldeweyense	Glosense	
				10.94	Glosense		
Middle Oxfordian	Transversarium	Elisabethae	10	10.44	Ilovaiskii	Tenuiserratum	Middle Oxfordian
		Buckmani	9	9.75	Blakei		
				9.5	Tenuiserratum		
	Plicatilis	Arkelli	8	8.5	Maltonense	Densiplicatum	
		Ouatius	7	6	Vertebrale		
		Patturatensis	6				
Lower Oxfordian	Cordatum	Cordatum	5	5	Cordatum	Cordatum	Lower Oxfordian
		Costicardia	4	4	Costicardia		
		Bukowskii	3	3	Bukowskii		
	Mariae	Praecordatum	2	2	Praecordatum	Mariae	
		Scarburgense	1	1	Scarburgense		
Up. Callov. (pars)	Lamberti (pars)	Lamberti	0	0	Lamberti	Lamberti (pars)	Up. Callov. (pars)

Fig. 2. Correlation between Submediterranean and (Sub)Boreal ammonite zonal schemes of the uppermost Callovian–lowermost Upper Kimmeridgian (after Głowniak et al., 2010; Matyja and Wierzbowski, 2000; Wierzbowski et al., 2013; Wierzbowski and Matyja, 2014; Scherzinger et al., 2016). Position of the base of each stratigraphical division is given in stratigraphical unit scale based on the assumed equal duration of Submediterranean ammonite subchrons.

composition of carbonate fossils can, thus, serve as a tool for evaluating their preservation state; particularly the concentrations of Mn < 100 ppm, Fe < 200 ppm, and Sr > 800 ppm are usually regarded as characteristic of well-preserved Jurassic belemnite rostra (see Nunn et al., 2009; Price and Rogov, 2009; Nunn and Price, 2010; Price and Teece, 2010; Wierzbowski and Rogov, 2011; Alberti et al., 2012b; Wierzbowski et al., 2013; Price et al., 2015; Wierzbowski, 2015; Arabas, 2016). Diagenetic Mn^{2+} ions are also an activator of orange-red cathodoluminescence in calcites, which is indicative of the alteration under reducing conditions (Marshall, 1992; Savard et al., 1995).

Newly collected mid-Kimmeridgian belemnite samples are characterized by the lack of luminescence and very low Mn (≤20 ppm) and Fe (≤33 ppm) as well as high Sr (≥1040 ppm; Table 1) concentrations. Their minor and trace element contents is similar to those of older belemnite material from the Russian Platform (cf. Wierzbowski and Rogov, 2011; Wierzbowski et al., 2013). Archival and new belemnite materials selected for the clumped isotope analyses show exceptionally low concentrations of Mn (≤ 9 ppm) and Fe (≤20 ppm) as well as high contents of Sr (≥824 ppm). Low contents of Mn and Fe in studied samples, which are buried in dark, often organic rich sediments, contradict suggestions that belemnite rostra might have been originally porous and cemented during early marine diagenesis (cf. Benito et al., 2016; Hoffmann et al., 2016; see also Supplementary Data 2). In addition, pervasive calcite cementation of fossils could not have occurred in fine-grained siliciclastic sediments of low permeability and carbonate content, which predominate in the Jurassic of the Russian Platform.

Aragonite is metastable and uncommon in Mesozoic deposits. Diagenetic alteration of aragonite mollusc shells results in the alteration of their microstructure and gradual transformation into calcite (cf. Brand, 1989; Dauphin and Denis, 1990; Anderson et al., 1994; Wierzbowski and Joachimski, 2007; Cochran et al., 2010; Wierzbowski and Rogov, 2011). Wierzbowski and Rogov (2011) and Wierzbowski et al. (2013) have documented that ammonite shells studied for oxygen and carbon isotope ratios, and presently for clumped isotope composition (Table 1), are composed of pure aragonite (≥ 99%) and show well-preserved shell microstructure.

Although the physical and chemical screening methods of the preservation state of calcium carbonate are well-established in a case of oxygen and carbon isotope studies the solid-state reordering of C—O bonds in the carbonate lattice can affect its Δ_{47} values without discernible microstructure and chemical changes. Recent studies of Passey and Henkes (2012), and Henkes et al. (2014) imply that Δ_{47} values of calcite preserve at burial temperatures below 100–120 °C. Models of Stolper and Eiler (2015) suggest, however, that calcites can undergo small decreases in their Δ_{47} values at temperatures of 80–100 °C. The clumped isotope composition of metastable aragonite is also very susceptible to the bond re-ordering and aragonite Δ_{47} values have been experimentally modified at 100 °C in aqueous fluids (Staudigel and Swart, 2016; Ritter et al., 2017).

The geothermal gradient of the Russian Platform is low (0.7 to

2.5 °C/100 m), and is estimated to have been ca. 3 °C/100 m during the Jurassic and the Cretaceous (Bazhenova, 2008). As a consequence, catagenic processes of hydrocarbon generation (above 75 °C) are expected to have occurred in sediments buried below 2.5 km. They affected Precambrian deposits of the Russian Platform (Bazhenova, 2008). Jurassic sediments of the Russian Platform occur close to the Earth surface and there is no evidence that they were deeply buried. Organic matter present in the Upper Jurassic in the study area is immature as it is indicated by low T_{max} in Rock Eval analyses (Hantzpergue et al., 1998; Shchepetova and Rogov, 2013; and Supplementary Data 2). Very low thermal maturity of the organic matter from Oxfordian strata near Makar'ev is additionally proved by high concentrations of original biomolecules (Bushnev et al., 2006). The presence of metastable aragonite in the sediments studied and similar Δ_{47} values of calcite and metastable aragonite may also point to the low thermal alteration. Although organic aragonites transform into calcite on heating above 250 °C (Yoshioka and Kitano, 1985), the aragonite-calcite transformation in aqueous solutions, which are common in diagenetic environments, were observed in the temperature range of 50–175 °C (Bischoff, 1969; Ritter et al., 2017).

4.2. Clumped isotopes

Measured $\Delta_{47\ (CDES\ 25)}$ (± 1σ S.E.) values of belemnite rostra and ammonite shells range between 0.678(± 0.004) and 0.716(± 0.011)‰ (mean 0.695‰; Table 1, Supplementary Data 1). The 1σ S.E. of the $\Delta_{47\ (CDES\ 25)}$ measurements, calculated from 4 to 13 replicate analyses, is between ± 0.003 and ± 0.011‰ (mean ± 0.006‰). No significant trends in $\Delta_{47\ (CDES\ 25)}$ values of the investigated fossil groups (cylindroteuthid and mesohibolitid belemnites, and ammonites) are observed in the studied interval (Fig. 3).

4.3. Oxygen isotopes

Various fossil groups, which co-occur in the uppermost Callovian and the Oxfordian of the Russian Platform, are characterized by different $\delta^{18}O$ values (Fig. 3). Mesohibolitid belemnite rostra are reported to have lower $\delta^{18}O$ values than those of coeval cylindroteuthids (cf. Wierzbowski and Rogov, 2011; Wierzbowski et al., 2013). Ammonites are divided into two groups: one from the Callovian–Oxfordian boundary and the lower part of the Tenuiserratum Zone of the Middle Oxfordian with $\delta^{18}O$ values between 0.0 and 1.5‰ (mean of 0.8‰) and another one from the Densiplicatum Zone of the Middle Oxfordian and the Middle–Late Oxfordian boundary with much lower $\delta^{18}O$ values between −0.5 and −2.5‰ (mean of −1.3‰; Fig. 3). $\delta^{18}O$ values of aragonitic gastropod shells vary between 1.0 and 1.4‰ (Fig. 3).

The $\delta^{18}O$ values of cylindroteuthid belemnite rostra, whose record spans the whole studied interval, show a decreasing trend (Fig. 3; cf. Wierzbowski and Rogov, 2011; Wierzbowski et al., 2013). Their $\delta^{18}O$ values range from −0.6 to 2.8‰ (mean of 1.6‰) in the uppermost Callovian and the Lower–Middle Oxfordian (Fig. 3). The cylindroteuthid $\delta^{18}O$ values decrease gradually in the Upper Oxfordian–Lower Kimmeridgian. The lowest cylindroteuthid $\delta^{18}O$ values of −1.9 to −1.0‰ (mean of −1.4‰) are documented from the Lower–Upper Kimmeridgian boundary.

4.4. Correlation between isotope and chemical ratios of cylindroteuthids

Temporal trends and relationships between various isotope and chemical data can be studied within the cylindroteuthid dataset, which covers the whole interval from the uppermost Callovian to the lowermost Upper Kimmeridgian (Fig. 3). There is a weak ($R = 0.41$) but statistically significant (at 1% level) linear correlation between $\delta^{18}O$ and $\delta^{13}C$ values of cylindroteuthid rostra (Fig. 4A) and a strong correlation ($R = 0.83$) between their $\delta^{18}O$ values and Sr/Ca ratios (Fig. 4C). A very weak ($R = 0.26$) linear correlation, significant at 5% level, is observed between cylindroteuthid $\delta^{18}O$ values and Mg/Ca ratios (Fig. 4B). No correlation is, in turn, noticed between cylindroteuthid $\Delta_{47\ (CDES\ 25)}$ and both $\delta^{18}O$ values and elemental proxies ($R \leq 0.11$; Fig. 4D-F). There is also no discernible differentiation in the isotope and chemical composition of various genera of studied cylindroteuthid belemnites.

5. Discussion

5.1. Water temperatures

A remarkable decrease (ca. 3‰) in $\delta^{18}O$ values of cylindroteuthid belemnite rostra (Fig. 3; see also Dromart et al., 2003; Wierzbowski and Rogov, 2011; Wierzbowski et al., 2013), if treated solely as a result of a temperature increase, may point to a warming of bottom waters of the Middle Russian Sea of ca. 12 °C during the Oxfordian and the Kimmeridgian. Differentiation of oxygen isotope compositions of various fossils (nektobenthic cylindroteuthid and mesohibolitid belemnites, and nektonic ammonites) from the Russian Platform is, in turn, regarded as a result of the presence of a significant thermal gradient in the water column of the Middle Russian Sea (Wierzbowski and Rogov, 2011; Wierzbowski et al., 2013).

The Middle Russian Sea was a huge and shallow epicontinental basin, whose salinities may have varied during the Jurassic, along with changes in the local palaeobathymetry, circulation patterns and connections with the open Tethys Ocean and the land-locked Boreal Sea (Fig. 5). Therefore, palaeotemperature reconstructions for this area based on the assumed constant water salinity and seawater $\delta^{18}O$ value should be treated with caution (Wierzbowski et al., 2013). Nevertheless, a Late Oxfordian–Early Kimmeridgian bottom water warming of 6.5–9.0 °C was suggested for the Middle Russian Sea as based on the changes in $\delta^{18}O$ values and Sr/Ca ratios of cylindroteuthid belemnite rostra (Wierzbowski et al., 2013).

Recent clumped isotope studies based on well-preserved carbonate fossils have proved the applicability of this method for the reconstruction of conditions of Mesozoic marine and brackish environments (Dennis et al., 2013; Price and Passey, 2013; Tobin et al., 2014; Petersen et al., 2016). Obtained clumped isotope data are derived from exceptionally well-preserved fossils of the Russian Platform and are fully reliable. Similar clumped isotope temperatures of ca. 16 °C are recorded for the whole studied interval encompassing the uppermost Callovian–mid Kimmeridgian (Fig. 3). Observed temperature variations are broadly within the ranges of measurement errors (ca. ± 2.3 °C) and likely arise from a general scatter of data points, with a few outliers. Since studied fossils (belemnites and ammonites) are considered to have been nektobenthic and nektonic, respectively (cf. Anderson et al., 1994; Wierzbowski and Joachimski, 2007; Wierzbowski and Rogov, 2011; Wierzbowski et al., 2013), the calculated clumped temperatures are expected to be relevant to bottom and intermediate waters of the Middle Russian Sea.

The studied basin was sensitive to a climate change due to its shallow, epicontinental character and location in mid-latitudes (40–45°N; Thierry et al., 2000) The constant clumped isotope temperatures evidence, therefore, long-term stability of the latest Middle Jurassic–Late Jurassic climate. The measured temperature of ca. 16 °C is a few degrees centigrade higher than modern average seawater temperatures (8.0 and 11.4 °C) at 100 m depth in the 40°N and 45°N, respectively (Locarnini et al., 2013). This may be a result of a warmer and more equable Jurassic climate and the absence of cold bottom water masses. It is worth noting that the calculated clumped isotope temperatures are within the range of previously reported belemnite clumped isotope temperatures (13–19 °C) for the lowermost Cretaceous of the sub-polar Urals (Price and Passey, 2013).

The calculated clumped isotope temperatures of the Middle Russian Sea for the latest Callovian–earliest Late Kimmeridgian (i.e. the Lamberti–Mutabilis time period; Fig. 3) challenge the previous

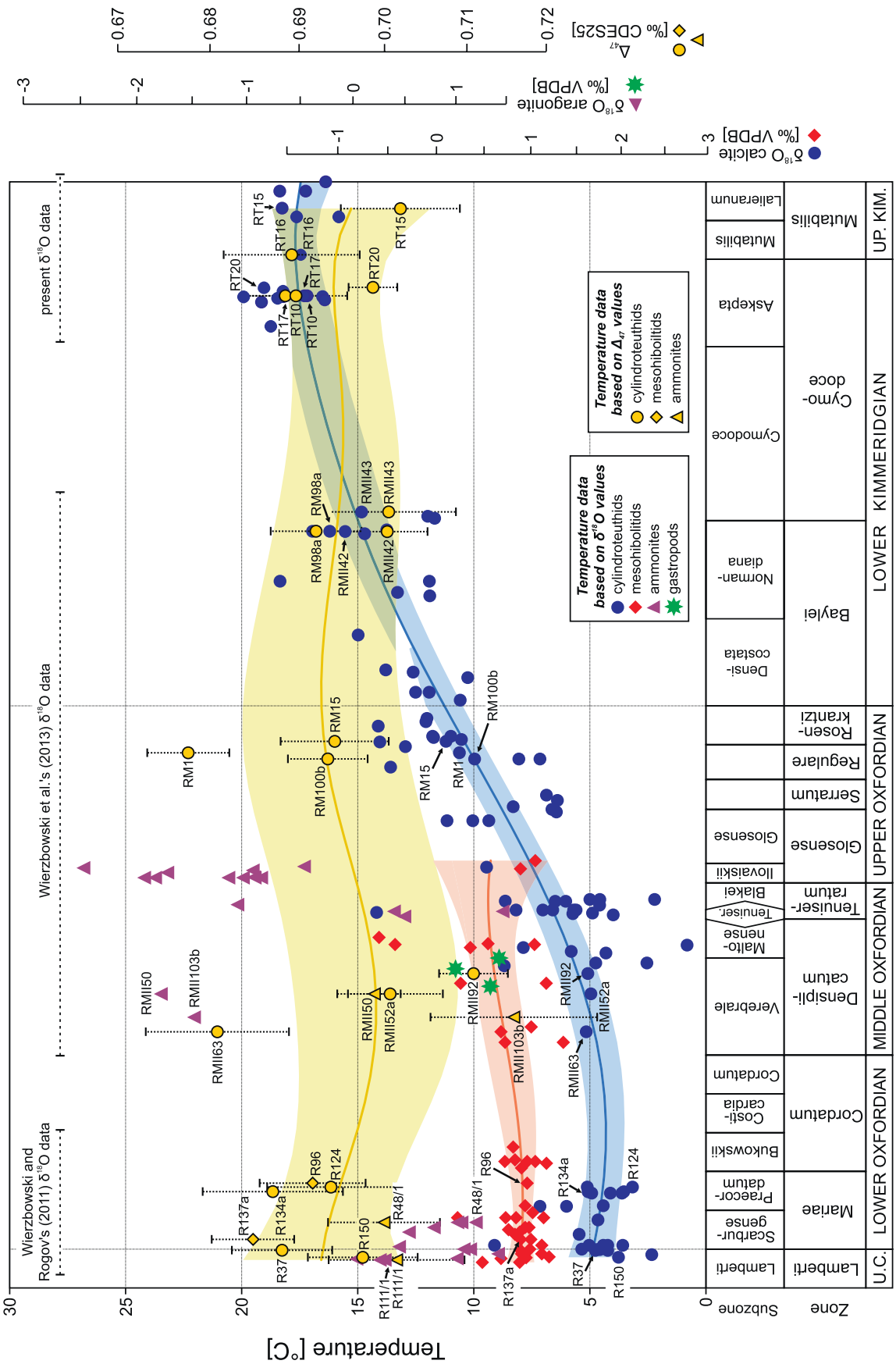

(caption on next page)

Fig. 3. Isotope data and palaeotemperatures calculated from $\delta^{18}O$ and $\Delta_{47\ (CDES\ 25)}$ values of well-preserved calcareous fossils from the Middle–Upper Jurassic (the uppermost Callovian–lowermost Upper Kimmeridgian) of the Russian Platform. Temperature data points derived from $\delta^{18}O$ and $\Delta_{47\ (CDES\ 25)}$ values of the same samples are marked with sample numbers. Smoothed curves and corresponding 95% confidence intervals (blue, red, and yellow areas) are generated using a locally weighted second order polynomial regression with a bandwidth of 5 stratigraphical units, i.e., ca. 0.3 Myr (cf. Chaudhuri and Marron, 1999). The $\delta^{18}O$ values are compiled from Wierzbowski and Rogov (2011), Wierzbowski et al. (2013) and from this study (see marked data ranges). (For interpretation of the references to colour in this figure legend, the reader is referred to the web version of this article.)

interpretation of the carbonate $\delta^{18}O$ signal. Prominent temporal variations in the cylindroteuthid belemnite $\delta^{18}O$ values of the Russian Platform (Fig. 3) are likely due to $\delta^{18}O_{water}$ and salinity variations. In addition, the clumped isotope data suggest that the previously postulated thermal stratification of the Middle Russian Sea (cf. Wierzbowski and Rogov, 2011; Wierzbowski et al., 2013) was apparent and arising from salinity stratification of the water column.

The positive correlation observed between $\delta^{18}O$ and $\delta^{13}C$ values of the studied fossils could either result from significant salinity fluctuations in marginal marine environments (Surge et al., 2001, 2003; Swart et al., 2001) or be related to kinetic effects (McConnaughey, 1989a, 1989b: McConnaughey et al., 1997; Auclair et al., 2003). It is, however, possible that a moderate positive correlation between $\delta^{18}O$ and $\delta^{13}C$ values of Russian cylindroteuthid belemnites (Fig. 4A) is a result of a more or less casual coincidence between a Kimmeridgian period of decreased belemnite $\delta^{18}O$ values in the Russian Platform and a global fall in $\delta^{13}C$ values of marine carbonates after the Middle Oxfordian positive carbon isotope excursion (cf. Wierzbowski et al., 2013; Wierzbowski, 2015).

Mg/Ca and Sr/Ca ratios of brackish waters remain relatively

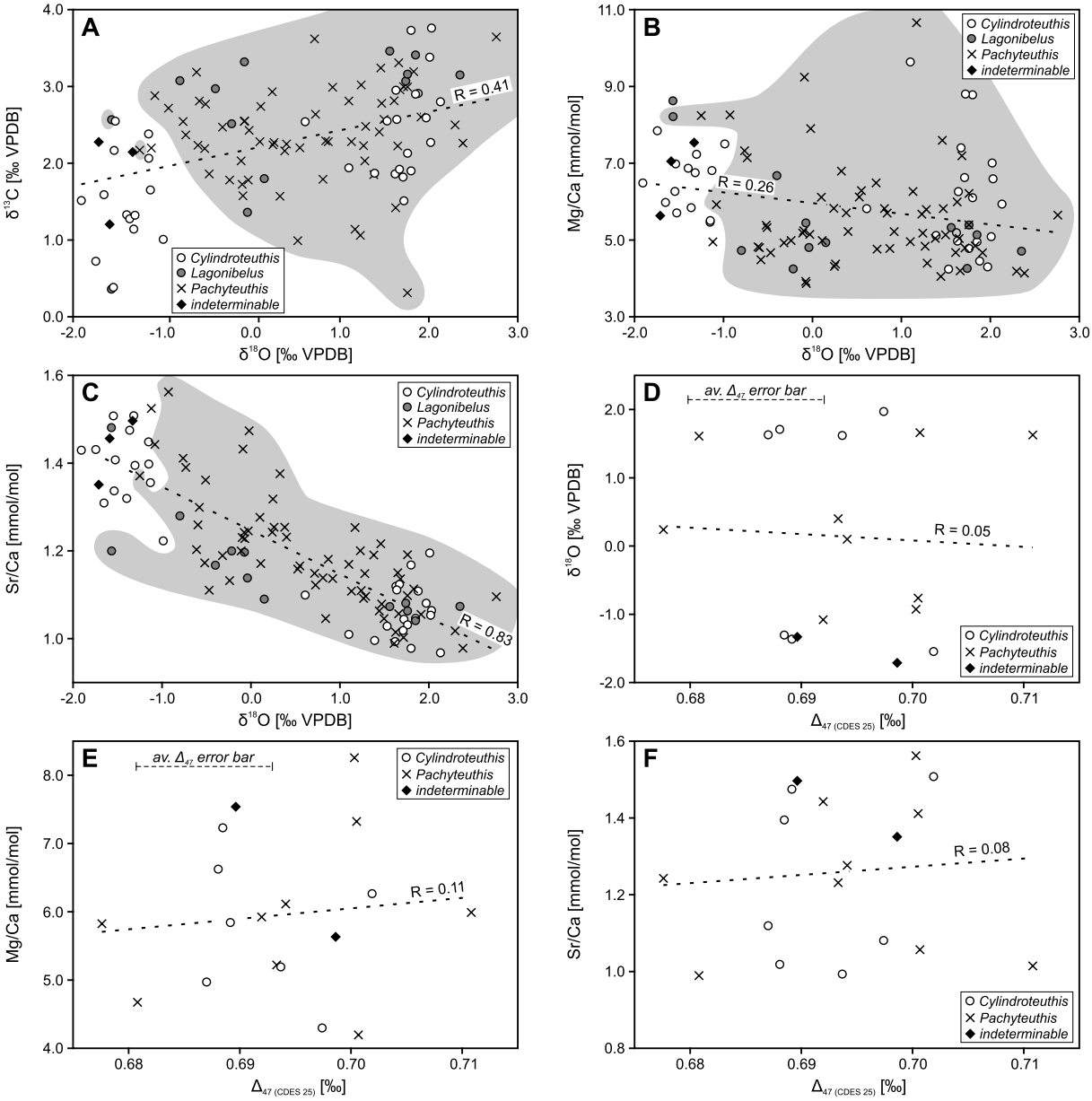

Fig. 4. Correlation between isotope values and elemental ratios of cylindroteuthid belemnite rostra from the Middle–Upper Jurassic (the uppermost Callovian–lowermost Upper Kimmeridgian) of the Russian Platform. Shaded areas represent datasets from Wierzbowski and Rogov (2011), and Wierzbowski et al. (2013).

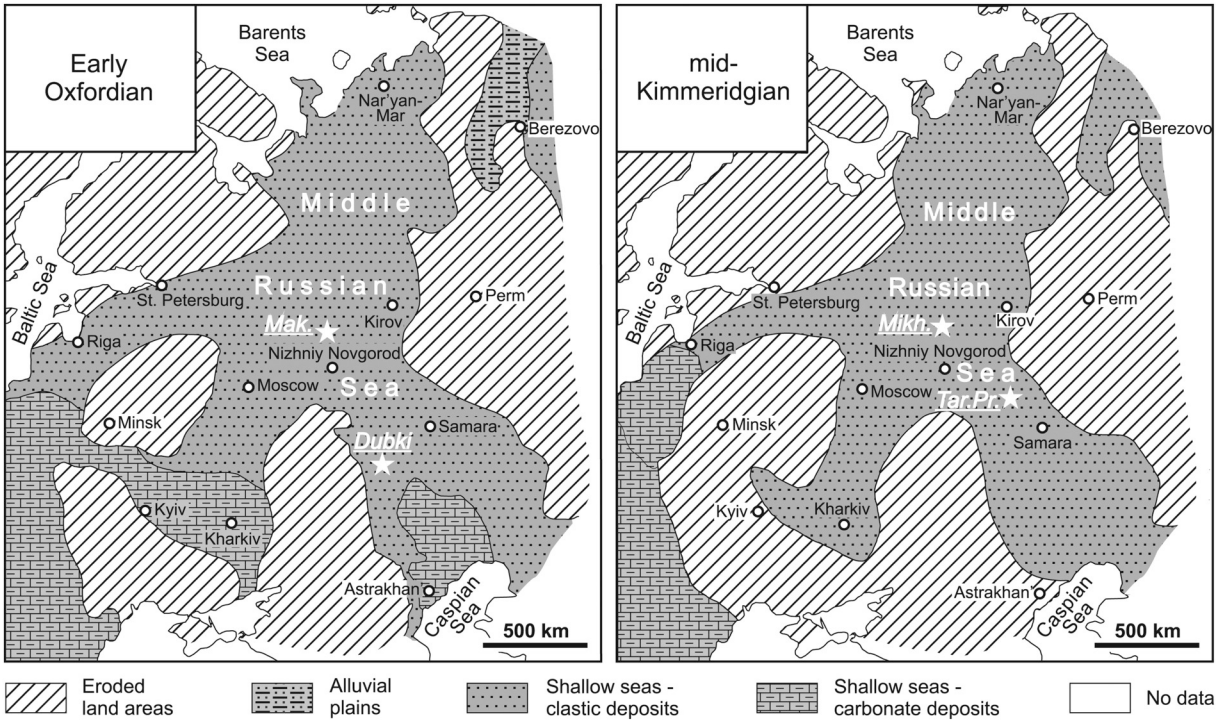

Fig. 5. Palaeogeography of the Russian Platform and adjacent areas during the Early Oxfordian and mid-Kimmeridgian (after Sazonova and Sazonov, 1967; Matyja and Wierzbowski, 1995; Lyyurov, 1996; Wierzbowski et al., 2015).

constant at salinities above 10‰ and a salinity effect on the elemental ratios of molluscs is not significant (Dodd and Crisp, 1982; Surge and Lohmann, 2008; Wanamaker et al., 2008). Interestingly, Mg/Ca and Sr/Ca ratios of some belemnite groups are regarded as a temperature proxy (McArthur et al., 2000, 2007b; Bailey et al., 2003; Rosales et al., 2004; Nunn and Price, 2010; Malkoč and Mutterlose, 2010; Armendáriz et al., 2013), whereas other authors suggest their relationship with biofractionation processes (McArthur et al., 2007a; Wierzbowski and Joachimski, 2009; Stevens et al., 2017; Ullmann and Pogge von Strandmann, 2017). A very weak negative correlation is observed between cylindroteuthid Mg/Ca ratios and $\delta^{18}O$ values (Fig. 4B). A slight, hardly discernible, increase of Mg/Ca ratios from ca. 5.2 to ca. 6.5 mmol/mol is concomitant with a huge decrease of belemnite $\delta^{18}O$ values, of ca. 3‰, within the entire dataset (Fig. 4B). According to the belemnite Mg/Ca temperature relationship of Nunn and Price (2010), Eq. (4) the observed rise in Mg/Ca ratio of cylindroteuthid belemnite rostra may be a response to an increase of ambient water temperature of ca. 2 °C. This also contradicts the temperature dependence of belemnite $\delta^{18}O$ values across the studied interval.

$$T(^{\circ}C) = \ln [(Mg/Ca)/1.2]/0.11 \quad (4)$$

The weak correlation between cylindroteuthid Mg/Ca ratios and $\delta^{18}O$ values, along with a little change in the Mg/Ca ratios, suggests that other factors controlled magnesium uptake of belemnite rostra. They may be related to temporal variations in water chemistry. Such explanation is plausible as the Mg/Ca ratio of seawater is considered to increase slightly in the Late Jurassic (Hardie, 1996; Dickson, 2004). The studied strata were deposited during a geological time of ca. 10 Ma (cf. Ogg et al., 2012, 2016; Wierzbowski et al., 2017), which is long enough to record a temporal change of global seawater Mg/Ca ratio.

Investigations of modern planktonic foraminifers, brachiopods and bivalves (Lea et al., 1999; Lorrain et al., 2005; Kısakürek et al., 2008; Freitas et al., 2012; Butler et al., 2015; Ullmann et al., 2017) indicate that the temperature sensitivity of Sr/Ca ratio of biogenic calcites is much weaker than the temperature sensitivity of the Mg/Ca ratio. In addition, prominent changes in the seawater Sr/Ca ratio, concomitant with $^{87}Sr/^{86}Sr$ variations, occurred during the Early and the Middle Jurassic (Ullmann et al., 2013). As the lowest seawater Sr/Ca ratio, which coincides with Phanerozoic minimum of the $^{87}Sr/^{86}Sr$ ratio, is postulated for the Middle–Late Jurassic transition (Ullmann et al., 2013) it is probable that the ratio increased after this turning point. The temporal change of the cylindroteuthid Sr/Ca ratio and its correlation with local record of belemnite $\delta^{18}O$ values (Fig. 4C; see also Wierzbowski et al., 2013) may, thus, be interpreted as arising from global variations in strontium and calcium concentrations in seawater. This explanation of cylindroteuthid Sr/Ca variations differs from that of Wierzbowski et al. (2013) but is in agreement with the lack of significant fluctuations of bottom water temperatures of the Middle Russian Sea during the latest Callovian–Kimmeridgian deduced from clumped isotopes.

Little variability in measured $\Delta_{47\ (CDES\ 25)}$ values along with significant standard errors of the measurements (Fig. 4E, F) precludes assessment if Mg/Ca and Sr/Ca ratios of cylindroteuthid calcite were controlled, to some degree, by the ambient water temperature during biomineralization processes.

5.2. Water $\delta^{18}O$ values

Clumped and oxygen isotope data allow calculation of $\delta^{18}O$ values of water from which calcium carbonate was precipitated. The $\delta^{18}O_{water}$ values of the Middle Russian Sea calculated from the cylindroteuthid data gradually decrease from ca. 2.0‰ at the Callovian–Oxfordian transition to ca. -1.4‰ VSMOW at the Early–Late Kimmeridgian transition (Fig. 6). Water $\delta^{18}O$ values calculated from Lower Oxfordian mesohibolitid data are ca. 0.5‰ lower than those of coeval cylindroteuthids. Ammonite data from the uppermost Callovian–Middle Oxfordian translate, in turn, into distinctly lower $\delta^{18}O_{water}$ values (from −4.0 to −0.1‰ VSMOW).

The $\delta^{18}O_{water}$ values for the Callovian–Oxfordian transition calculated from cylindroteuthid data are very heavy assuming the average seawater isotope composition of ca. -1‰ VSMOW (Shackleton and Kennett, 1975) as distinctive of the Jurassic world, which was devoid of

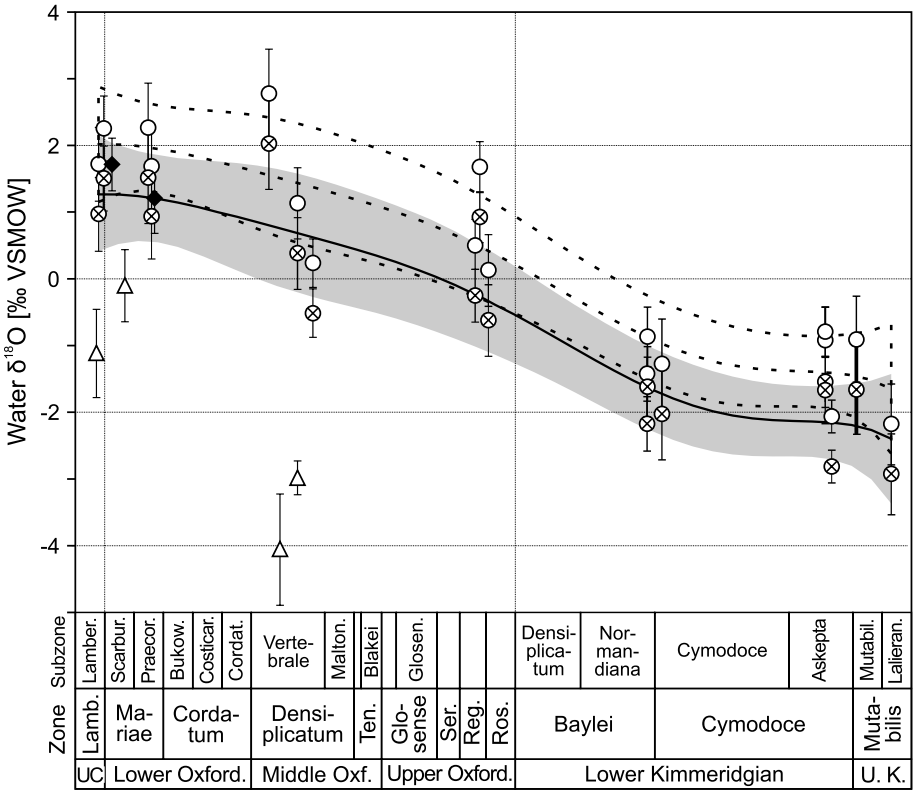

Fig. 6. Water $\delta^{18}O$ values of the Middle Russian Sea estimated on the basis of oxygen and clumped isotope compositions of studied fossils and cylindroteuthid $\delta^{18}O$ values corrected for the −0.75‰ offset from mesohibolitid values (see text). Smoothed curves and corresponding 95% confidence intervals, calculated using locally weighted polynomial regression, represent cylindroteuthid (dashed) and corrected cylindroteuthid (shaded) $\delta^{18}O_{water}$ salinity trends.

continental glaciation. Seawater $\delta^{18}O$ values above +2‰ VSMOW are not observed in modern oceans (Craig and Gordon, 1965; LeGrande and Schmidt, 2006; Rohling, 2013). Increases in $\delta^{18}O_{water}$ values, higher than 2‰ above average composition of seawater, are also not predicted in models for the ice-free mid-Cretaceous (Zhou et al., 2008). Recent studies have, however, shown that palaeotemperatures calculated from $\delta^{18}O$ values of cylindroteuthid rostra are 1–3 °C lower than those derived from co-occurring bivalve shells (Anderson et al., 1994; Mettam et al., 2014; Price et al., 2015). There is also a discrepancy between oxygen isotope palaeotemperatures derived from calcitic rostra and aragonitic phragmocones of the same cylindroteuthid belemnites (Price et al., 2015). Phragmocones are depleted in ^{18}O, which may apparently suggest higher temperature of precipitation. Although a reason for this discrepancy is not clear, it seems that temperatures calculated from $\delta^{18}O$ values of cylindroteuthid rostra, using commonly applied isotope equations, are slightly underestimated. On the other hand, palaeotemperatures derived from $\delta^{18}O$ values of Jurassic mesohibolitid rostra are in better agreement with those from coeval bivalves and brachiopods (Wierzbowski and Joachimski, 2007; Price and Page, 2008; Price and Teece, 2010; Wierzbowski, 2015). If presently reported mesohibolitid $\delta^{18}O$ values from the uppermost Callovian–Middle Oxfordian (Fig. 3) of the Russian Platform reflect oxygen isotope fractionation predicted by Friedman and O'Neil (1977), the offset between coeval mesohibolitid and cylindroteuthid oxygen isotope data (ca. 0.75‰) may suggest a necessity of the correction of the cylindroteuthid dataset.

$\delta^{18}O_{water}$ values calculated using the cylindroteuthid data, corrected for the 0.75‰ offset from mesohibolitid data, are distinctly lower. They average 1.2‰ for the Callovian–Oxfordian transition, and ca. -2.1‰ VSMOW for the Early–Late Kimmeridgian transition (Fig. 6). The corrected cylindroteuthid data probably better reflect true variations in ancient seawater chemistry of bottom waters of the Middle Russian Sea showing a gradual decrease in $\delta^{18}O_{water}$ values and salinity during the Oxfordian and the Early Kimmeridgian.

5.3. Water salinity

Bottom water salinity of the Middle Russian Sea can be estimated using the $\delta^{18}O_{water}$ values based on corrected cylindroteuthid data and a universal salinity–$\delta^{18}O$ relation models for marine basins given by Railsback et al. (1989), which take into account effects of freshwater runoff (Eq. (5)) and evaporation (Eq. (6)). The two equations are used for salinity calculations below and above the normal marine, respectively.

$$\delta^{18}O_{water} = \delta^{18}O_0 + \Delta_{fw}/S_0^* (S_{water} - S_0) \quad (5)$$

where $\delta^{18}O_0$ is the average oxygen isotope composition of Jurassic seawater assumed as −1‰ VSMOW (after Shackleton and Kennett, 1975), Δ_{fw} is a difference between $\delta^{18}O$ values of average seawater and local meteoric water, and S_0 is average seawater salinity.

$$\delta^{18}O_{water} = \delta^{18}O_0 + m_0^*(S_{water} - S_0) \quad (6)$$

where $\delta^{18}O_0$ is the average oxygen isotope composition of Jurassic seawater assumed as −1‰ VSMOW (after Shackleton and Kennett, 1975), m_0 is an evaporative enrichment parameter being a relation between $\delta^{18}O$ and salinity observed in evaporative basins, and S_0 is average seawater salinity.

Average Late Jurassic seawater salinity of 34‰, $\delta^{18}O_{precipitation}$ at 45°N equal to −9‰ VSMOW, and an evaporative enrichment parameter of 0.35‰VSMOW per 1 salinity per mil may be deduced from their modern equivalents, according to Railsback et al. (1989). Alternatively, another average salinity of 39.4‰ and $\delta^{18}O_{precipitation}$ at 45°N of −7.5‰ VSMOW may be assumed for the Late Jurassic according to data given by Hay et al. (2006) and Zhou et al. (2008), respectively. Assumption of the higher average salinity in the second model results in a need of adjustment of evaporative enrichment parameter (m_0) to a wider salinity range. Its calculated value is 0.31‰VSMOW per 1 salinity per mil.

The constructed models suggest higher, than average, salinity of bottom waters of the Middle Russian Sea during the latest

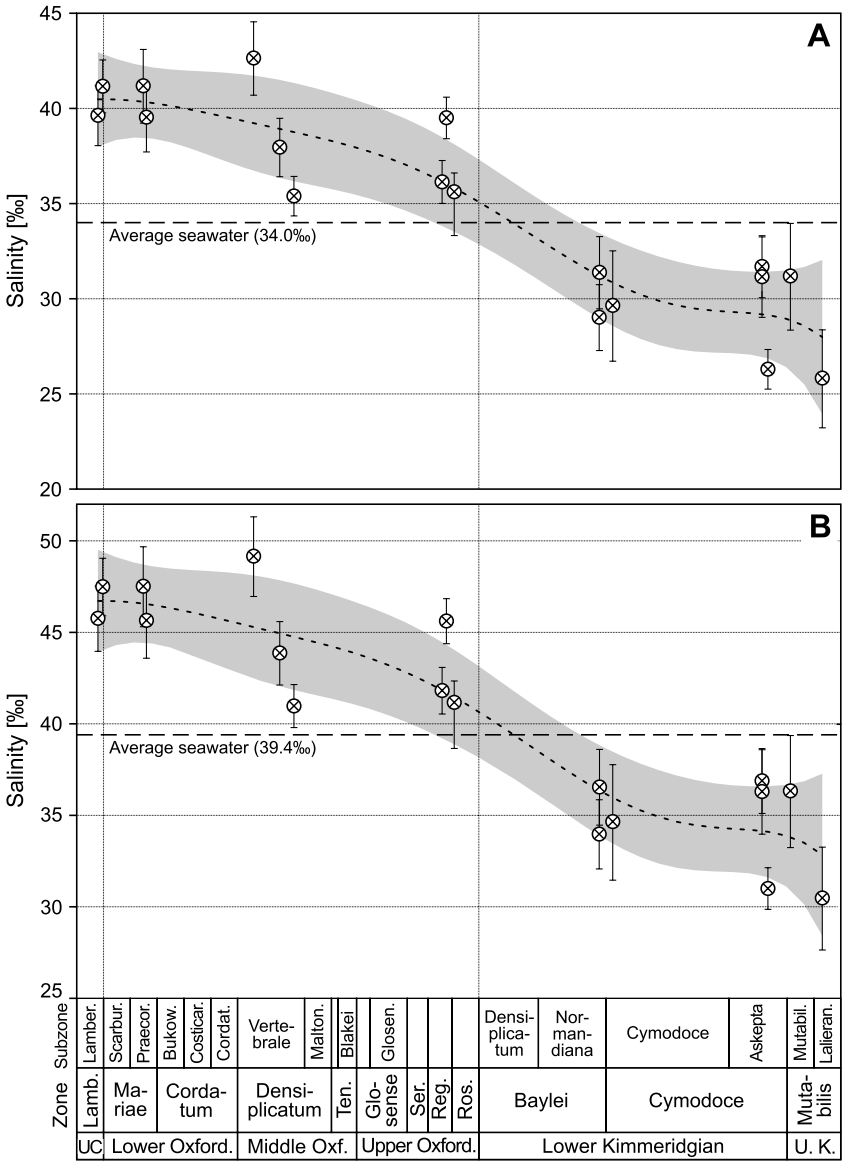

Fig. 7. Palaeosalinity variations of the Middle Russian Sea during the latest Callovian–earliest Late Kimmeridgian modelled from clumped and corrected oxygen isotope values of cylindroteuthid belemnite rostra (applying the fractionation equations of Friedman and O'Neil, 1977, and Wacker et al., 2014). Average seawater salinity of 34.0‰ (model A) and 39.4‰ (model B) is accepted for Late Jurassic oceans after Railsback et al. (1989) and Hay et al. (2006), respectively. Smoothed curves of salinity trends and corresponding 95% confidence intervals, are calculated using locally weighted polynomial regression.

Callovian–Middle Oxfordian and freshening of the basin during the Late Oxfordian–earliest Kimmeridgian (Fig. 7). Although the modelled data are tentative because of i) uncertainty of published clumped isotope temperature scales (cf. Wacker et al., 2014) and considerable standard errors of measurements of $\Delta_{47\ (CDES\ 25)}$ values, ii) problems with the estimation of real oxygen isotope fractionation for cylindroteuthid belemnites rostra (cf. Price et al., 2015), and iii) assumption of non-actualistic values of seawater salinity and oxygen isotope composition of precipitation for the Jurassic (cf. Hay et al., 2006; Zhou et al., 2008), the data provide strong evidence for salinity variations in the Subboreal Realm. Waters of the Middle Russian Sea may have been characterized by increased salinities during the latest Callovian–Middle Oxfordian because of diminished freshwater influx and the presence of saline, subtropical, Tethyan waters. A general decrease in sea level after the worldwide Middle–Late Jurassic transition highstand (cf. Sazonova and Sazonov, 1967; Norris and Hallam, 1995; Hallam, 2001; Wierzbowski et al., 2009, 2013) may have contributed to the enhanced freshwater runoff, and the limitation of oceanic water exchange with the restricted Middle Russian Sea. This probably led to a decrease in salinity and water $\delta^{18}O$ values of this basin. The decrease is likely recorded in $\delta^{18}O$ values of carbonate fossils from the Russian Platform, whose fall was previously interpreted as an evidence for the prolonged period of warm Kimmeridgian–Volgian climate (Riboulleau et al., 1998; Price and Rogov, 2009). Coeval oxygen isotope data from other (Sub)boreal basins i.e. Scotland, Northern Siberia (Nunn et al., 2009; Nunn and Price, 2010; Žak et al., 2011) suggest that the Kimmeridgian–Volgian decrease in carbonate $\delta^{18}O$ values is a common feature in this palaeobiogeographical province. In addition, clumped isotope data imply that previously postulated thermal stratification of the Middle Russian Sea (cf. Wierzbowski and Rogov, 2011; Wierzbowski et al., 2013) was apparent and resulting from salinity and $\delta^{18}O$ value stratification of the water column. Unfortunately, relatively scarce and scattered $\delta^{18}O_{water}$ values (Fig. 6) calculated from ammonite data do not allow precise estimation of the salinity of subsurface waters, where ammonites lived (cf. Wierzbowski et al., 2013).

The increasing restriction of the Middle Russian Sea during the Late

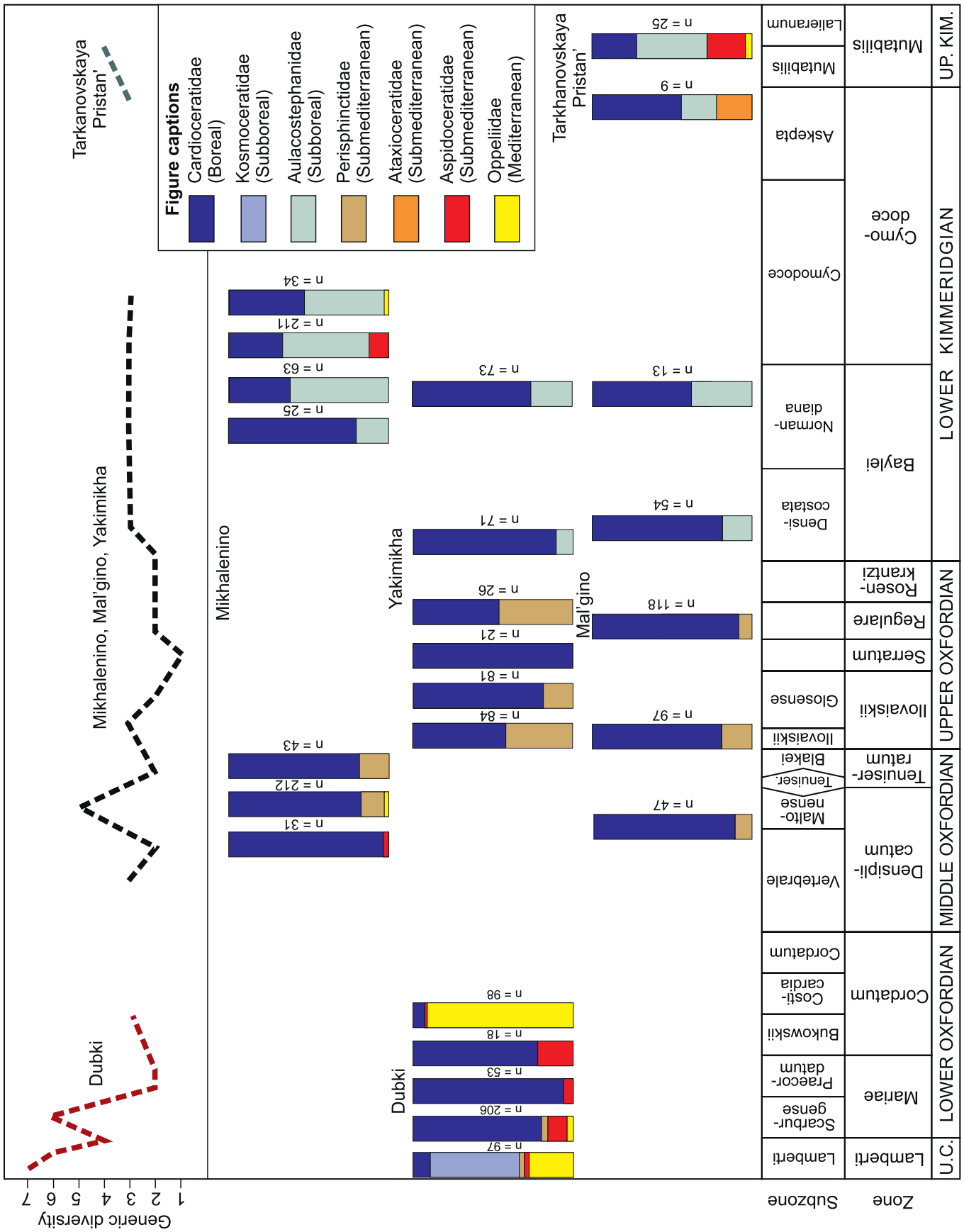

Fig. 8. Changes in latest Callovian–earliest Late Kimmeridgian ammonite assemblages of the Russian Platform. Ammonite diversity is calculated based on number of macroconchiate genera in cases when different genera names are used for micro- and macroconchs of the same ammonite.

Oxfordian–earliest Kimmeridgian is substantiated by a fall in $\varepsilon_{Nd\ (t)}$ values of local sediments, which is linked to an increasing rate of neodymium derived from adjacent Precambrian cratons (Dera et al., 2015). Limitation of water circulation and salinity stratification of the Middle Russian Sea may have contributed to the formation of oxygen depleted bottom layer and the deposition of black shales rich in organic matter, which are common in the Russian Platform starting from the Middle–Upper Oxfordian boundary (Hantzpergue et al., 1998; Zakharov et al., 2017). Black shale layers occur in the studied sections of the Russian Platform in the Maltonense Subzone of the Densiplicatum Zone of the uppermost Middle Oxfordian, in the Ilovaiskii Subzone of the Glosense Zone of the lowermost Upper Oxfordian, and in the Lalieranum Subzone of the Mutabilis Zone of the lowermost Upper Kimmeridgian (Głowniak et al., 2010; Wierzbowski et al., 2013; Rogov et al., 2017; Zakharov et al., 2017; see also Supplementary Data 2). A local organic rich layer is additionally found in the lowermost Kimeridgian (the Densicostata Subzone of the Baylei Zone) of the Kostroma Region of Russia (Zakharov et al., 2017). Interestingly, black shales are even more widespread and thick in the uppermost Kimmeridgian–Volgian of the Russian Platform (Hantzpergue et al., 1998; Shchepetova et al., 2011; Zakharov et al., 2017). Organic rich strata are also common in the uppermost Oxfordian–Lower Tithonian of NW Europe (Hantzpergue et al., 1998; Morgans-Bell et al., 2001; Smelror et al., 2001) and attributed to restricted water circulation during sea-level lowstand (Mutterlose et al., 2003). Weakening of water movement and inflow of freshwaters into Subboreal basins in the Late Jurassic is consistent with postulated models of deposition of the organic rich beds under permanent or seasonal stratification of the water column (cf. Tyson et al., 1979; Oschmann, 1991) or during a spread of stagnant deep waters in submarine depressions (cf. Wignall and Hallam, 1991).

5.4. Changes in cephalopod assemblages

Significant decrease in salinity of the Middle Russian Sea, indicated by clumped and oxygen isotope data, should have affected local marine faunas. Although the suggested drop of salinity lies within a common range of marine salinities, its impact on biota could be noticeable constituting a major reason for periods of occurrences of a mixed Boreal–Mediterranean and endemic Boreal cephalopod faunas in the study area (cf. Wierzbowski and Rogov, 2011; Głowniak et al., 2010).

Cephalopods do not tolerate large decreases in salinity because of the salt sensitivity of the hemocyanin in their blood (Mangum, 1991). Mangold and Boletzky (1988) show that no modern cephalopod survives at salinities lower than 15‰ or higher than 45‰ although some species are moderately tolerant to salinity variations. For example, *Lolliguncula brevis* occurred at salinities between 17 and 38‰ (Zuev and Nesis, 1971) while *Sepia officinalis* is caught in regions characterized by fluctuations in salinity from 20 to 35.5‰ (Guerra and Castro, 1988). It should be noted that areas characterized either by low or high salinities are poor in cephalopods (Zuev and Nesis, 1971). Response of extinct ammonites to low or high salinity remains unclear, although a general relationship between their diversity and salinities is suggested. Some ammonites, e.g. some Triassic ceratitids, are interpreted to be tolerant to high salinities (Westermann, 1996). Ammonites from the Late Cretaceous Western Interior Seaway of North America are, in turn, interpreted to have occurred at a wide range of salinities between 20 and 35‰ (Cochran et al., 2003). Hallam (1969) argue that reduced salinity in Boreal seas was a key factor responsible for the diversity contrast between Tethyan and Boreal faunas. This view is criticized by Stevens (1971) who suggests climatic zonation as a dominant factor responsible for differentiation of marine faunas.

Callovian–Kimmeridgian ammonite faunas of the study areas are characterized by the mixed origin and consist of Boreal, Subboreal, Submediterranean and Mediterranean taxa (Zakharov and Rogov, 2003; Głowniak et al., 2010; Wierzbowski and Rogov, 2011; Kiselev et al., 2013). Ammonite assemblages have been studied in sections sampled for clumped isotopes and two additional sections (Mal'gino and Yakimikha) located in the Kostroma Region of Russia (Fig. 8).

Nearly all studied uppermost Callovian–Oxfordian ammonite faunas are dominated by Boreal cardioceratids except for an assemblage of the Bukowskii Subzone of the Cordatum Zone (Lower Oxfordian, the Dubki section), which is crowded by Mediterranean oppeliids (Wierzbowski and Rogov, 2011; Kiselev et al., 2013; Fig. 8). Ammonites of the Submediterrranean origin occur in the Lower and the Middle Oxfordian. Starting from the Middle–Upper Oxfordian boundary Submediterrranean ammonites decline in frequency, and they are missing from the uppermost Oxfordian (Głowniak et al., 2010; Fig. 8). Lowermost Kimmeridgian assemblages are dominated by dwarf Boreal *Plasmatites* with the admixture of Subboreal aulacostephanids; only in a short interval near the Baylei–Cymodoce boundary an assemblage with relatively common Submediterranean faunal elements (*Aspidoceras*, *Lingulaticeras*) is recognized (Głowniak et al., 2010; Rogov, 2017; Fig. 8). The Lower–Upper Kimmeridgian boundary studied recently in the southern Tatarstan is also characterized by the presence of Submediterranean taxa. They are represented by *Crussoliceras* spp. in the uppermost Cymodoce Zone and by *Aspidoceras* spp. in the Mutabilis Zone (Rogov et al., 2017; Fig. 8). Taking into account the absence of aspidoceratids in the Mutabilis Subzone of the Subboreal succession of Western Europe, it may be concluded that these ammonites penetrated in the Middle Russian Sea via a southern strait which connected it with Caucasian margin of the Tethys.

Ammonite assemblages of the Russian Platform are characterized by a drop of diversity near the Callovian–Oxfordian boundary. Appearance of Submediterranean ammonites in some intervals possibly reflect changes in water circulation (cf. Rogov et al., 2017). Oscillations in ammonoid assemblages of the Russian Platform are not consistent with palaeotemperature data based on oxygen isotopes (cf. Riboulleau et al., 1998; Dromart et al., 2003; Price and Rogov, 2009; Wierzbowski et al., 2013). Late Oxfordian–Early Kimmeridgian ammonite assemblages of the Russian Platform are strongly dominated by Boreal and Subboreal taxa, which is in conflict with a temperature rise postulated previously based on the oxygen isotope composition of carbonate fossils. Observed changes in the ammonite assemblages are, however, in general agreement with a gradual decrease of salinity detected by present clumped and oxygen isotope analyses.

The Mediterranean mesohibolitid belemnites of the Russian Platform are represented by the genus *Hibolithes* (Gustomesov, 1976). They are characterized by small size (maximal diameter of ca. 8 mm) compared to the much bigger *Hibolithes* rostra found in Central or Southern Europe (Gustomesov, 1976; Wierzbowski et al., 2013). Occurrences of *Hibolithes* belemnites in the Russian Platform become discontinuing at the Middle–Upper Oxfordian boundary; they disappear totally in the Upper Oxfordian (Rogov, 2003; Wierzbowski et al., 2013). This is consistent with postulated restriction and a decrease in salinity of the Middle Russian Sea.

5.5. Changes in ostracod and other microfossil assemblages

Uppermost Callovian–Lower Kimmeridgian ostracod fauna of the Russian Platform was studied in detail by Tesakova (2008) and Tesakova et al. (2012). Ostracods occur at wide ranges of salinity and cannot be used as an indicator of moderate salinity oscillations. Despite attempts of the reconstruction of variations of seawater temperatures based on the distribution of ostracod faunas (see Tesakova, 2014b) there are still problems with interpretation of thermal preferences of cosmopolitan taxa; observed changes in distribution of ostracods may also be affected by sea-level fluctuations.

An approach to the reconstruction of relative depth of the basin based on analysis of ostracod communities has been done by Tesakova (2014a). The lower boundary of the upper sublittoral zone (below 50 m), which is penetrated by visible light and grown by seaweeds, is usually inhabited by large-sized benthic ostracods (carapace length of

0.48–1.2 mm). Another small-shelled ostracod assemblage (carapace length 0.25–0.32 mm) is typical of deposit feeders, which occur at all depths but predominate in the middle part of the shelf and in deeper environments (Yasuhara et al., 2009; Tesakova, 2014a). The shallow-water environments can, thus, be recognized based on high abundance (70–90%) of large-shelled ostracods.

The Callovian–Kimmeridgian assemblage of large-sized ostracods of the Russian Platform consists of the following genera: *Amphicythere*, *Balowella*, *Bythoceratina*, *Cytherella*, *Fastigatocythere*, *Fuhrbergiella*, *Galliaecytheridea*, *Klentnicella*, *Lophocythere*, *Neurocythere*, *Patellacythere*, *Platylophocythere*, *Progonocythere*, *Sabacythere* and *Schuleridea*. Small-sized ostracods are, in turn, represented by *Acrocythere*, *Cytheropteron*, *Dicrorygma* (*Orthorygma*), *Eucytherura*, *Exophthalmocythere*, *Polycope*, *Rubracea*, *Paracypris*, *Pontocypris*, *Pontocyprella*, *Paranotacythere*, *Micropneumatocythere*, *Pedicythere*, *Procytherura* and *Tethysia*. The common Callovian–Kimmeridgian small-sized ostracods including *Cytheropteron*, *Eucytherura* and *Pedicythere* also occur in modern seas being characterized of the lower sublitoral and the deeper zones (cf. Mostafawi et al., 2010).

Variations in relative diversity of small-shelled and large-shelled assemblages studied in the Dubki and the Mikhalenino sections are shown (Fig. 9). A predominance of the shallow-water environment is inferred for the latest Callovian due to the high abundance of large-sized ostracods in the Lamberti Zone. Since the beginning of the Oxfordian relative diversity of small-sized genera grows drastically. The small-sized ostracods prevail in the Oxfordian and the lowermost Kimmeridgian. It reveals deep-water settings of the studied part of the Middle Russian Sea in this time period. Shallowing, marked by increasing diversity of large-sized ostracods, began in the latest Baylei Chron and is evident in the Cymodoce Chron of the Early Kimmeridgian. The large-sized ostracods also predominate in the Volgian of the Russian Platform (Tesakova, 2017; Ustinova and Tesakova, 2017). The sea-level fall and the restriction of the Middle Russian Sea during the Early Kimmeridgian are, thus, suggested based on the ostracod fauna.

Worth noting is also the distribution of other microfossils in the Russian Platform. Planktonic foraminifera are abundant in the Middle and the lowermost Upper Oxfordian of the Makar'ev and Mikhalenino section. They become rare in younger sediments and gradually disappear around the Oxfordian–Kimmeridgian boundary (Ustinova, 2012; Colpaert et al., 2016). Studied assemblages of calcareous nannoplankton from the Moscow region show a general decline in abundance and a noticeable decrease in number of cosmopolitic *Watznaueria* spp. in the uppermost Oxfordian (Ustinova, 2009).

Microfossil data substantiate the validity of present interpretations of temporal changes in salinity and circulation of the Middle Russian Sea based on isotope proxies. They are not consistent with previous views about the existence of a few short-term falls in sea-level of the basin during the Oxfordian, which might have overlapped the long-term period of high sea-level (cf. Sahagian et al., 1996).

6. Conclusions

Clumped isotope analyses of chemically and thermally well-preserved belemnite rostra and ammonite shells from the Russian Platform have allowed calculation of absolute temperatures of seawater of the Middle Russian Sea and verification of previously presented opinions on latest Middle–Late Jurassic palaeoenvironmental and palaeoclimatic variations.

The clumped isotope data indicate constant temperatures of water of the Middle Russian Sea of ca. 16 °C in the course of the latest Callovian–earliest Late Kimmeridgian. This documents long-term stability of the Late Jurassic climate and challenges previous opinions on a short-term cooling at the Callovian–Oxfordian transition and a pronounced warming during the Late Oxfordian–Early Kimmeridgian. Minor variations in belemnite Mg/Ca ratios and major variations in their Sr/Ca ratios are presently interpreted as reflecting secular variations in global seawater chemistry rather, than temperatures of belemnite growth.

The clumped and oxygen isotope data derived from cylindroteuthid belemnites, which occur continuously in the studied sediments, enable calculation of variations in $\delta^{18}O_{water}$ values and estimation of fluctuations in salinity of the Middle Russian Sea around the Middle–Late Jurassic transition. The data show the presence of waters of possibly slightly increased salinities during the latest Callovian–Middle

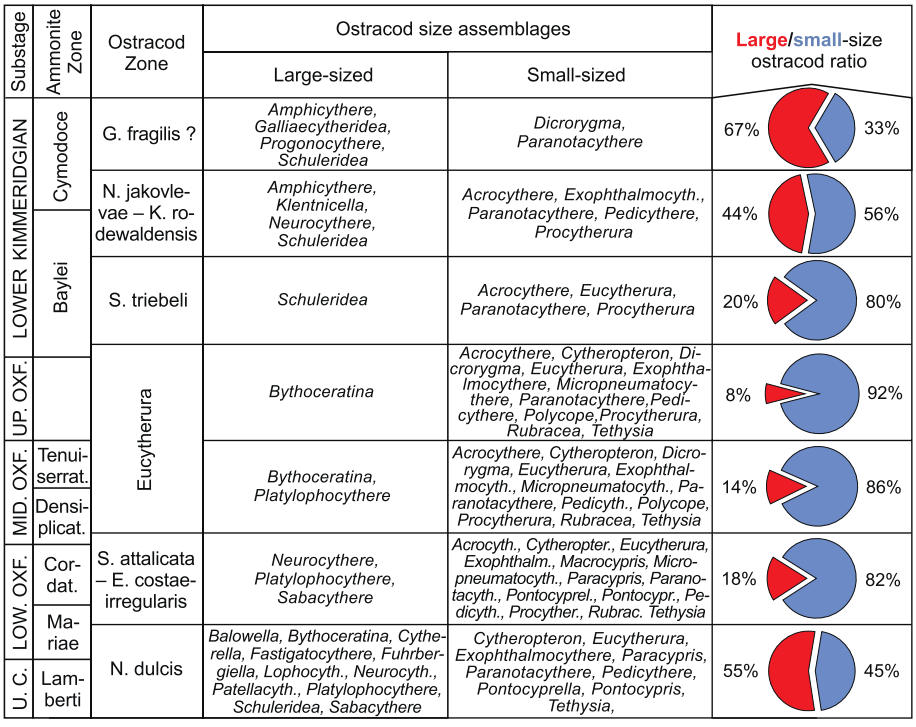

Fig. 9. Variations in number of large-sized and small-sized ostracods in the Oxfordian–Lower Kimmeridgian of the Dubki and the Mikhalenino sections.

Oxfordian and a gradual decrease in salinity (of ca. 12‰) during the Late Oxfordian–earliest Kimmeridgian. The observed change may be connected with the inflow of saline, subtropical waters from the Tethys Ocean during the sealevel highstand at the Middle–Late Jurassic transition and a subsequent period of progressive isolation of the Middle Russian Sea resulting in freshening of its waters. This is consistent with increasing provincialism of local macro- and microfauna in the Late Oxfordian–Early Kimmeridgian.

Similar circulation changes probably occurred in all Subboreal basins of Europe. They are manifested by decreases in $\delta^{18}O$ values of carbonate fossils, decreases in $\varepsilon_{Nd\ (t)}$ sediment values, and increasing faunal provincialism. The restriction of epeiric Subboreal basins, diminishing water circulation and freshwater input may have contributed to temporal bottom water anoxia and widespread sedimentation of Upper Jurassic organic-rich facies.

Acknowledgements

This study was supported by the grant no. 2014/13/B/ST10/02511 of the National Science Centre, Poland and received funding from the European Union's Horizon 2020 research and innovation program under the Marie Skłodowska-Curie grant no. 643084 (BASE-LiNE Earth). The paleontological part of this study, conducted by Mikhail A. Rogov and Ekaterina M. Tesakova, was financed by the Russian Foundation for Basic Research (grants no. 18-05-01070, and no. 18-05-00501) and followed research plans of the Geological Institute of RAS (projects no. 0135-2018-0035, and 0135-2018-0036) and the M.V. Lomonosov Moscow State University (project no. AAAA-A16-116033010096-8). We are indebted to Alexei Ippolitov for kind determination of taxonomy of belemnite rostra from the Lower–Upper Kimmeridgian boundary of the Tarkhanovskaya Pristan' section. Alvaro Fernandez and an anonymous reviewer are thanked for valuable reviews and suggested improvements.

Appendix A. Supplementary data

Supplementary data to this article can be found online at https://doi.org/10.1016/j.gloplacha.2018.05.014.

References

Abbink, O., Targarona, J., Brinkhuis, H., Visscher, H., 2001. Late Jurassic to earliest Cretaceous palaeoclimatic evolution of southern North Sea. Glob. Planet. Change 30, 231–256. https://doi.org/10.1016/S0921-8181(01)00101-1.

Alberti, M., Fürsich, F.T., Pandey, D.K., 2012a. The Oxfordian stable isotope record ($\delta^{18}O$, $\delta^{13}C$) of belemnites, brachiopods, and oysters from the Kachchh Basin (western India) and its potential for palaeoecologic, palaeoclimatic, and palaeogeographic reconstructions. Palaeogeogr. Palaeoclimatol. Palaeoecol. 344-345, 49–68. https://doi.org/10.1016/j.palaeo.2012.05.018.

Alberti, M., Fürsich, F.T., Pandey, D.K., Ramkumar, M., 2012b. Stable isotope analyses of belemnites from the Kachchh Basin, western India: paleoclimatic implications for the Middle to Late Jurassic transition. Facies 58, 261–278. https://doi.org/10.1007/s10347-011-0278-9.

Anderson, T.F., Popp, B.N., Williams, A.C., Ho, L.-Z., Hudson, J.D., 1994. The stable isotopic records of fossils from the Peterborough Member, Oxford Clay Formation (Jurassic) UK: palaeoenvironmental implications. J. Geol. Soc. Lond. 151, 125–138. https://doi.org/10.1144/gsjgs.151.1.0125.

Arabas, A., 2016. Middle–Late Jurassic stable isotope records and seawater temperature variations: new palaeoclimate data from marine carbonate and belemnite rostra (Pieniny Klippen Belt, Carpathians). Palaeogeogr. Palaeoclimatol. Palaeoecol. 446, 284–294. https://doi.org/10.1016/j.palaeo.2016.01.033.

Armendáriz, M., Rosales, I., Bádenas, B., Piñuela, L., Aurell, M., García-Ramos, J.-C., 2013. An approach to estimate Lower Jurassic seawater oxygen-isotope composition using $\delta^{18}O$ and Mg/Ca ratios of belemnite calcites (Early Pliensbachian, northern Spain). Terra Nova 25, 439–445. https://doi.org/10.1111/ter.12054.

Auclair, A.-C., Joachimski, M.M., Lécuyer, C., 2003. Deciphering kinetic, metabolic and environmental controls on stable isotope fractionations between seawater and the shell of *Terebratalia transversa* (Brachiopoda). Chem. Geol. 202, 59–78. https://doi.org/10.1016/s0009-2541(03)00233-x.

Bailey, T.R., Rosenthal, Y., McArthur, J.M., van de Schootbrugge, B., Thirlwall, M.F., 2003. Paleoceanographic changes of the Late Pliensbachian–Early Toarcian interval: a possible link to the genesis of an Oceanic Anoxic Event. Earth Planet. Sci. Lett. 212, 307–320. https://doi.org/10.1016/S0012-821X(03)00278-4.

Bajnai, D., Fiebig, J., Tomašovych, A., Milner Garcia, S., Rollion-Bard, C., Raddatz, J., Löffler, N., Primo-Ramos, C., Brand, U., 2018. Assessing kinetic fractionation in brachiopod calcite using clumped isotopes. Sci. Rep. 8, 533. https://doi.org/10.1038/s41598-017-17353-7.

Bazhenova, T.K., 2008. Problem of petroleum potential of basal horizons in the basins of ancient platforms in aspect of their katagenetic evolution. Petrol. Geol. 3, 1–21 (In Russian).

Benito, M.I., Reolid, M., Viedma, C., 2016. On the microstructure, growth pattern and original porosity of belemnite rostra: insights from calcite Jurassic belemnites. J. Iber. Geol. 42, 201–226. https://doi.org/10.5209/rev_JIGE.2016.v42.n2.53232.

Bischoff, J.L., 1969. Temperature controls on aragonite-calcite transformation in aqueous solution. Am. Mineral. 54, 149–155.

Böhm, F., Joachimski, M.M., Dullo, W.-C., Eisenhauer, A., Lehnert, H., Reitner, J., Wörheide, G., 2000. Oxygen isotope fractionation in marine aragonite of coralline sponges. Geochim. Cosmochim. Acta 64, 1695–1703. https://doi.org/10.1016/S0016-7037(99)00408-1.

Bonifacie, M., Calmels, D., Eiler, J.M., Horita, J., Chaduteau, C., Vasconcelos, C., Agrinier, P., Katz, A., Passey, B.H., Ferry, J.M., Bourrand, J.-J., 2017. Calibration of the dolomite clumped isotope thermometer from 25 to 350 °C, and implications for a universal calibration for all (Ca, Mg, Fe)CO_3 carbonates. Geochim. Cosmochim. Acta 200, 255–279. https://doi.org/10.1016/j.gca.2016.11.028.

Brand, U., 1989. Aragonite–calcite transformation based on Pennsylvanian mollusks. Bull. Geol. Soc. Am. 101, 377–390. https://doi.org/10.1130/0016-7606(1989)101<0377:ACTBOP>2.3.CO;2.

Brand, U., Veizer, J., 1980. Chemical diagenesis of a multicomponent carbonate system–1: trace elements. J. Sediment. Petrol. 50, 1219–1236. https://doi.org/10.1306/212F7BB7-2B24-11D7-8648000102C1865D.

Brigaud, B., Pucéat, E., Pellenard, P., Vincent, B., Joachimski, M.M., 2008. Climatic fluctuations and seasonality during the Late Jurassic (Oxfordian–Early Kimmeridgian) inferred from $\delta^{18}O$ of Paris Basin oyster shells. Earth Planet. Sci. Lett. 273, 58–67. https://doi.org/10.1016/j.epsl.2008.06.015.

Bushnev, D.A., Shchepetova, E.V., Lyyurov, S.V., 2006. Organic geochemistry of Oxfordian carbon-rich sedimentary rocks of the Russian Plate. Lithol. Miner. Resour. 41, 423–434. https://doi.org/10.1134/s0024490206050038.

Butler, S., Bailey, T.R., Lear, C.H., Curry, G.B., Cherns, L., McDonald, I., 2015. The Mg/Ca-temperature relationship in brachiopod shells: calibrating a potential palaeoseasonality proxy. Chem. Geol. 397, 106–117. https://doi.org/10.1016/j.chemgeo.2015.01.009.

Chaudhuri, P., Marron, J.S., 1999. SiZer for exploration of structures in curves. J. Am. Stat. Assoc. 94, 807–823. https://doi.org/10.2307/2669996.

Cochran, J.K., Kallenberg, K., Landman, N.H., Harries, P.J., Weinreb, D., Turekian, K.K., Beck, A.J., Cobban, W.A., 2010. Effect of diagenesis on the Sr, O and C isotope composition of Late Cretaceous mollusks from the Western Interior Seaway of North America. Am. J. Sci. 310, 69–88. https://doi.org/10.2475/02.2010.01.

Cochran, J.K., Landman, N.H., Turekian, K.K., Michard, A., Schrag, D.P., 2003. Paleoceanography of the Late Cretaceous (Maastrichtian) Western Interior Seaway of North America: evidence from Sr and O isotopes. Palaeogeogr. Palaeoclimatol. Palaeoecol. 191, 45–64. https://doi.org/10.1016/S0031-0182(02)00642-9.

Colpaert, C., Nikitenko, B., Khafaeva, S., Wall, A.F., 2016. The evolution of Late Callovian to Early Kimmeridgian foraminiferal associations from the central part of the Russian Sea (Makar'yev section, Volga River Basin, Russia). Palaeogeogr. Palaeoclimatol. Palaeoecol. 451, 97–109. https://doi.org/10.1016/j/palaeo.2016.03.014.

Coplen, T.B., Kendall, C., Hopple, J., 1983. Comparison of stable isotope reference samples. Nature 302, 236–238. https://doi.org/10.1038/302236a0.

Craig, H., Gordon, L.I., 1965. Deuterium and oxygen 18 variations in the ocean and the marine atmosphere. In: Tongiorgi, E. (Ed.), Proceedings of the Spoleto Conference on Stable Isotopes in Oceanographic Studies and Paleotemperatures. Consiglio Nazionale delle Ricerche, Laboratorio de Geologia Nucleare, Pisa, pp. 9–130.

Dauphin, Y., Denis, A., 1990. Analyse microstructurale des tests de mollusques du Callovien de Lukow (Pologne) – Comparaison de l'etat de conservation de quelques types structuraux majeurs. Rev. Paléobiol. 9, 27–36.

Defliese, W.F., Hren, M.T., Lohmann, K.C., 2015. Compositional and temperature effects of phosphoric acid fractionation on Δ_{47} analysis and implications for discrepant calibrations. Chem. Geol. 396, 51–60. https://doi.org/10.1016/j.chemgeo.2014.12.018.

Dennis, K.J., Affek, H.P., Passey, B.H., Schrag, D.P., Eiler, J.M., 2011. Defining an absolute reference frame for 'clumped' isotope studies of CO_2. Geochim. Cosmochim. Acta 75, 7117–7131. https://doi.org/10.1016/j.gca.2011.09.025.

Dennis, K.J., Cochran, J.K., Landman, N.H., Schrag, D.P., 2013. The climate of the Late Cretaceous: new insights from the application of the carbonate clumped isotope thermometer to Western Interior Seaway macrofossils. Earth Planet. Sci. Lett. 362, 51–65. https://doi.org/10.1016/j.epsl.2012.11.036.

Dera, G., Prunier, J., Smith, P.L., Haggart, J.W., Popov, E., Guzhov, A., Rogov, M., Delsate, D., Thies, D., Cuny, G., Pucéat, E., Charbonnier, G., Bayon, G., 2015. Nd isotope constraints on ocean circulation, paleoclimate, and continental drainage during the Jurassic breakup of Pangea. Gondwana Res. 27, 1599–1615. https://doi.org/10.1016/j.gr.2014.02.006.

Dickson, J.A.D., 2004. Echinoderm skeletal preservation: calcite–aragonite seas and the Mg/Ca ratio of Phanerozoic oceans. J. Sediment. Res. 74, 355–365. https://doi.org/10.1306/112203740355.

Dodd, J.R., Crisp, E.L., 1982. Non-linear variation with salinity of Sr/Ca and Mg/Ca ratios in water and aragonitic bivalve shells and implications for paleosalinity studies. Palaeogeogr. Palaeoclimatol. Palaeoecol. 38, 45–56. https://doi.org/10.1016/0031-0182(82)90063-3.

Dromart, G., Garcia, J.-P., Gaumet, F., Picard, S., Rousseau, M., Atrops, F., Lecuyer, C., Sheppard, S.M.F., 2003. Perturbation of the carbon cycle at the Middle/Late Jurassic

transition: geological and geochemical evidence. Am. J. Sci. 303, 667–707. https://doi.org/10.2475/ajs.303.8.667.
Eiler, J.M., 2011. Paleoclimate reconstruction using carbonate clumped isotope thermometry. Quaternary Sci. Rev. 30, 3575–3588. https://doi.org/10.1016/j.quascirev.2011.09.001.
Fiebig, J., Hofmann, S., Niklas, L., Lüdecke, T., Methner, K., Wacker, U., 2016. Slight pressure imbalances can affect accuracy and precision of dual inlet-based clumped isotope analysis. Isot. Environ. Healt 52, 12–28. https://doi.org/10.1080/10256016.2015.1010531.
Finnegan, S., Bergmann, K., Eiler, J.M., Jones, D.S., Fike, D.A., Eisenman, I., Hughes, N.C., Tripati, A.K., Fischer, W.W., 2011. The magnitude and duration of Late Ordovician–Early Silurian glaciation. Science 331, 903–906. https://doi.org/10.1126/science.1200803.
Freitas, P.S., Clarke, L.J., Kennedy, H., Richardson, C.A., 2012. The potential of combined Mg/Ca and $\delta^{18}O$ measurements within the shell of the bivalve *Pecten maximus* to estimate seawater $\delta^{18}O$ composition. Chem. Geol. 291, 286–293. https://doi.org/10.1016/j.chemgeo.2011.10.023.
Friedman, I., O'Neil, J.R., 1977. Compilation of stable isotope fractionation factors of geochemical interest, Data of Geochemistry, 6th edn. Geochemical Survey Professional Paper, pp. KK1–KK12.
Ghosh, P., Adkins, J., Affek, H., Balta, B., Guo, W., Shauble, E.A., Schrag, D., Eiler, J.M., 2006. ^{13}C–^{18}O bonds in carbonate minerals: a new kind of paleothermometer. Geochim. Cosmochim. Acta 70, 1439–1456. https://doi.org/10.1016/j.gca.2005.11.014.
Głowniak, E., Kiselev, D.N., Rogov, M., Wierzbowski, A., Wright, J.K., 2010. The Middle Oxfordian to lowermost Kimmeridgian ammonite succession at Mikhalenino (Kostroma District) of the Russian Platform, and its stratigraphical and palaeobiogeographical importance. Vol. Jur. 8, 5–48.
Guerra, A., Castro, B.G., 1988. On the life cycle of *Sepia officinalis* (Cephalopoda, Sepioidea) in the ria de Vigo (NW Spain). Cah. Biol. Mar. 29, 395–405. https://doi.org/10.21411/CBM.A.96C24EDF.
Guo, W., Mosenfelder, J.L., Goddard, W.A., Eiler, J.M., 2009. Isotopic fractionations associated with phosphoric acid digestion of carbonate minerals: insights from first-principles theoretical modeling and clumped isotope measurements. Geochim. Cosmochim. Acta 73, 7203–7225. https://doi.org/10.1016/j.gca.2009.05.071.
Gustomesov, V.A., 1976. O pozdneyurskikh belemnitakh roda *Hibolithes* Russkoy Platformy. Paleontol. Zh. 4, 51–60 (In Russian).
Hallam, A., 1969. Faunas realms and facies in the Jurassic. Palaeontology 12, 1–18.
Hallam, A., 2001. A review of the broad pattern of Jurassic sea-level changes and their possible causes in the light of current knowledge. Palaeogeogr. Palaeoclimatol. Palaeoecol. 167, 23–37. https://doi.org/10.1016/S0031-0182(00)00229-7.
Hantzpergue, P., Baudin, F., Mitta, V., Olferiev, A., Zakharov, V., 1998. The Upper Jurassic of the Volga Basin: ammonite biostratigraphy and occurrence of organic-carbon rich facies. Correlations between boreal-subboreal and submediterranean provinces. In: Crasquin-Soleau, S., Barrier, E. (Eds.), Peri-Tethys Memoir 4. vol. 179. pp. 9–33 Epicratonic Basins of Peri-Tethyan Platforms. Mém. Mus. Natn. Hist. Nat.
Hardie, L.A., 1996. Secular variation in seawater chemistry: an explanation for the coupled secular variation in the mineralogies of marine limestones and potash evaporites over the past 600 m.Y. Geology 24, 279–283. https://doi.org/10.1130/0091-7613(1996)024<0279:svisca>2.3.co;2.
Hay, W.W., Migdisov, A., Balukhovsky, A.N., Wold, C.N., Flögel, S., Söding, E., 2006. Evaporites and the salinity of the ocean during the Phanerozoic: implications for climate, ocean circulation and life. Palaeogeogr. Palaeoclimatol. Palaeoecol. 240, 3–46. https://doi.org/10.1016/j.palaeo.2006.03.044.
Henkes, G.A., Passey, B.H., Wanamaker Jr., A.D., Grossman, E.L., Ambrose Jr., W.G., Carroll, M.L., 2013. Carbonate clumped isotope compositions of modern marine mollusk and brachiopod shells. Geochim. Cosmochim. Acta 106, 307–325. https://doi.org/10.1016/j.gca.2012.12.020.
Henkes, G.A., Passey, B.H., Grossmann, E.L., Shenton, B.J., Pérez-Huerta, A., Yancey, T.E., 2014. Temperature limits for preservation of primary calcite clumped isotope paleotemperatures. Geochim. Cosmochim. Acta 139, 362–382. https://doi.org/10.1016/j.gca.2014.04.040.
Hoffmann, R., Richter, D.K., Neuser, R.D., Jöns, N., Linzmeier, B.J., Lemanis, R.E., Fusseis, F., Xiao, X., Immenhauser, A., 2016. Evidence for a composite organic-inorganic fabric of belemnite rostra: implications for palaeoceanography and palaeoecology. Sediment. Geol. 341, 203–215. https://doi.org/10.1016/j.sedgeo.2016.06.001.
Imai, N., Terashima, S., Itoh, S., Ando, A., 1996. 1996 compilation of analytical data on nine GSJ geochemical reference samples, "sedimentary rock series". Geostand. Newslett. 20, 165–216. https://doi.org/10.1111/j.1751-908X.1996.tb00184.x.
Jenkyns, H.C., Schouten-Huibers, S., Sinninghe Damsté, J.S., 2012. Warm Middle Jurassic–Early Cretaceous high-latitude sea-surface temperatures from the Southern Ocean. Clim. Past 8, 215–226. https://doi.org/10.5194/cp-8-215-2012.
Kısakürek, B., Eisenhauer, A., Böhm, F., Garbe-Schönberg, D., Erez, J., 2008. Controls on shell Mg/Ca and Sr/Ca in cultured planktonic foraminiferan, *Globigerinides ruber* (white). Earth Planet. Sci. Lett. 273, 260–269. https://doi.org/10.1016/j/epsl.2008.06.026.
Kiselev, D., Rogov, M., Glinskikh, L., Guzhikov, A., Pimenov, M., Mikhailov, A., Dzyuba, O., Matveev, A., Tesakova, E., 2013. Integrated stratigraphy of the reference sections for the Callovian-Oxfordian boundary in European Russia. Vol. Jur. 11, 59–96.
Lea, D.W., Mashiotta, T.A., Spero, H.J., 1999. Controls on magnesium and strontium uptake in planktonic foraminifera determined by live culturing. Geochim. Cosmochim. Acta 63, 2369–2379. https://doi.org/10.1016/s0016-7037(99)00197-0.
Lécuyer, C., Picard, S., Garcia, J.P., Sheppard, S.M.F., Grandjean, P., Dromart, G., 2003. Thermal evolution of Tethyan surface waters during the Middle–Late Jurassic: evidence from $\delta^{18}O$ values of marine fish teeth. Paleoceanography 18, 1–16. https://doi.org/10.1029/2002pa000863.
LeGrande, A.N., Schmidt, G.A., 2006. Global gridded data set of the oxygen isotopic composition in seawater. Geophys. Res. Lett. 33, L12604. https://doi.org/10.1029/2006GL026011.
Locarnini, R.A., Mishonov, A.V., Antonov, J.I., Boyer, T.P., Garcia, H.E., Baranova, O.K., Zweng, M.M., Paver, C.R., Reagan, J.R., Johnson, D.R., Hamilton, M., Seidov, D., 2013. In: Levitus, S., Mishonov, A. (Eds.), World Ocean Atlas 2013. Volume 1: Temperature. NOAA Atlas NESDIS, pp. 1–40.
Lorrain, A., Gilikin, D.P., Paulet, Y.-M., Chauvaud, L., Le Mercier, A., Navez, J., André, L., 2005. Strong kinetic effects on Sr/Ca ratios in the calcitic bivalve *Pecten maximus*. Geology 33, 965–968. https://doi.org/10.1130/G22048.1.
Lyyurov, S.V., 1996. Yurskie Otlozheniya Severa Russkoy Plity. UrO RAN, Ekaterinburg, pp. 138 In Russian.
Malkoč, M., Mutterlose, J., 2010. The Early Barremian warm pulse and the Late Barremian cooling: a high-resolution geochemical record of the Boreal Realm. Palaios 25, 14–23. https://doi.org/10.2110/palo.2010.p09-029r.
Mangold, K., Boletzky, S.V., 1988. Mediterranean cephalopod fauna. In: Clarke, M.R., Trueman, E.R. (Eds.), The Mollusca. Paleontology and Neontology of Cephalopods 12. Academic Press, Inc, San Diego, New York, Berkeley, Boston, London, Sydney, Tokyo, Toronto, pp. 315–330. https://doi.org/10.1016/B978-0-12-751412-3.50025-5.
Mangum, C.P., 1991. Salt-sensitivity of the hemocyanin of eury- and stenohaline squids. Comp. Biochem. Physiol. A. 99, 159–161. https://doi.org/10.1016/0300-9629(91)90251-7.
Marshall, J.D., 1992. Climatic and oceanographic isotopic signals from the carbonate rock record and their preservation. Geol. Mag. 129, 143–160. https://doi.org/10.1017/s0016756800008244.
Matyja, B.A., Wierzbowski, A., 1995. Biogeographic differentiation of the Oxfordian and Early Kimmeridgian ammonite faunas of Europe, and its stratigraphic consequences. Acta Geol. Pol. 45, 1–8.
Matyja, B.A., Wierzbowski, A., 2000. Biostratigraphical correlations between the Subboreal Mutabilis Zone and the Submediterranean Upper Hypselocyclum – Divisum zones of the Kimmeridgian: new data from Northern Poland. Geores. Forum 6, 129–136.
McArthur, J.M., Donovan, D.T., Thirlwall, M.F., Fouke, B.W., Mattey, D., 2000. Strontium isotope profile of the Toarcian (Jurassic) oceanic anoxic event, the duration of ammonite biozones, and belemnite palaeotemperatures. Earth Planet. Sci. Lett. 179, 269–285. https://doi.org/10.1016/S0012-821X(00)00111-4.
McArthur, J.M., Doyle, P., Leng, M.J., Reeves, K., Williams, C.T., Garcia-Sanchez, R., Howarth, R.J., 2007a. Testing palaeo-environmental proxies in Jurassic belemnites: Mg/Ca, Sr/Ca, Na/Ca, $\delta^{18}O$ and $\delta^{13}C$. Palaeogeogr. Palaeoclimatol. Palaeoecol. 252, 464–480. https://doi.org/10.1016/j.palaeo.2007.05.006.
McArthur, J.M., Janssen, N.M.M., Reboulet, S., Leng, M.J., Thirlwall, M.F., van de Schootbrugge, B., 2007b. Palaeotemperatures, polar ice-volume, and isotope stratigraphy (Mg/Ca, $\delta^{18}O$, $\delta^{13}C$, $^{87}Sr/^{86}Sr$): the Early Cretaceous (Berriasian, Valanginian, Hauterivian). Palaeogeogr. Palaeoclimatol. Palaeoecol. 248, 391–430. https://doi.org/10.1016/j.paleo.2006.12.015.
McConnaughey, T.A., 1989a. ^{13}C and ^{18}O isotopic disequlibrium in biological carbonates: I. Patterns. Geochim. Cosmochim. Acta 53, 151–162. https://doi.org/10.1016/0016-7037(89)90282-2.
McConnaughey, T.A., 1989b. ^{13}C and ^{18}O isotopic disequlibrium in biological carbonates: II. *In vitro* simulation of kinetic isotope effects. Geochim. Cosmochim. Acta 53, 163–171. https://doi.org/10.1016/0016-7037(89)90283-4.
McConnaughey, T.A., Burdett, J., Whelan, J.F., Paull, C.K., 1997. Carbon isotopes in biological carbonates: respiration and photosynthesis. Geochim. Cosmochim. Acta 61, 611–622. https://doi.org/10.1016/s0016-7037(96)00361-4.
Mettam, C., Johnson, A.L.A., Nunn, E.V., Schöne, B.R., 2014. Stable isotope ($\delta^{18}O$ and $\delta^{13}C$) sclerochronology of Callovian (Middle Jurassic) bivalves (*Gryphaea* (*Bilobissa*) *dilobotes*) and belemnites (*Cylindroteuthis puzosiana*) from the Peterborough Member of the Oxford Clay Formation (Cambridgeshire, England): evidence of palaeoclimate, water depth and belemnite behaviour. Palaeogeogr. Palaeoclimatol. Palaeoecol. 399, 187–201. https://doi.org/10.1016/j.palaeo.2014.01.010.
Morgans-Bell, H.S., Coe, A.L., Hesselbo, S.P., Jenkyns, H.C., Weedon, G.P., Marshall, J.E.A., Tyson, R.V., Williams, C.J., 2001. Integrated stratigraphy of the Kimmeridge Clay Formation (Upper Jurassic) based on exposures and boreholes in south Dorset, UK. Geol. Mag. 138, 511–539. https://doi.org/10.1017/S0016756801005738.
Mostafawi, N., Nabavi, S.M., Moghaddasi, B., 2010. Ostracods from the Strait of Hormuz and Gulf of Oman, Northern Arabian Sea. Rev. Esp. Micropaleontol. 42, 243–265.
Mutterlose, J., Brumsack, H., Flögel, S., Hay, W., Klein, C., Langrock, U., Lipinski, M., Ricken, W., Söding, E., Stein, R., Swientek, O., 2003. The Greenland-Norwegian Seaway: a key area for understanding Late Jurassic to Early Cretaceous paleoenvironments. Paleoceanography 18, 1010. https://doi.org/10.1029/2001PA000625.
Norris, M.S., Hallam, A., 1995. Facies variations across the Middle–Upper Jurassic boundary in Western Europe and the relationship to sea-level changes. Palaeogeogr. Palaeoclimatol. Palaeoecol. 116, 189–245. https://doi.org/10.1016/0031-0182(94)00096-Q.
Nunn, E.V., Price, G.D., 2010. Late Jurassic (Kimmeridgian–Tithonian) stable isotopes ($\delta^{18}O$, $\delta^{13}C$) and Mg/Ca ratios: new paleoclimate data from Helmsdale, Northeast Scotland. Palaeogeogr. Palaeoclimatol. Palaeoecol. 292, 325–335. https://doi.org/10.1016/j.palaeo.2010.04.015.
Nunn, E.V., Price, G.D., Hart, M.B., Page, K.N., Leng, M.J., 2009. Isotopic signals from Callovian–Kimmeridgian (Middle–Upper Jurassic) belemnites and bulk organic carbon, Staffin Bay, Isle of Skye, Scotland. J. Geol. Soc. Lond. 166, 633–641. https://doi.org/10.1144/0016-76492008-067.
Ogg, J.G., Hinnov, L.A., Huang, C., 2012. Jurassic. In: Gradstein, F.M., Ogg, J.G., Schmitz, M., Ogg, G. (Eds.), The Geologic Time Scale. Elsevier, Amsterdam, Boston,

Heidelberg, London, New York, Oxford, Paris, San Diego, San Francisco, Singapore, Sydney, Tokyo, pp. 731–791.
Ogg, J.G., Ogg, G.M., Gradstein, F.M., 2016. A Concise Geologic Time Scale. Vol. 234 Elsevier, Amsterdam, Boston, Heidelberg, London, New York, Oxford, Paris, San Diego, San Francisco, Singapore, Sydney, Tokyo.
O'Neil, J.R., Clayton, R.N., Mayeda, T.K., 1969. Oxygen isotope fractionation in divalent metal carbonates. J. Chem. Phys. 51, 5547–5558. https://doi.org/10.1063/1.1671982.
Oschmann, W., 1991. Distribution, dynamics and palaeoecology of the Kimmeridgian (Upper Jurassic) shelf anoxia in Western Europe. In: Tyson, R.V., Pearson, T.H. (Eds.), Modern and Ancient Continental Shelf Anoxia, pp. 381–395. Geological Society Special Publication No. 58. https://doi.org/10.1144/GSL.SP.1991.058.01.24.
Passey, B.H., Henkes, G.A., 2012. Carbonate clumped isotope bond reordering and geospeedometry. Earth Planet. Sci. Lett. 351-352, 223–236. https://doi.org/10.1016/j.epsl.2012.07.021.
Petersen, S.V., Tabor, C.R., Lohmann, K.C., Poulsen, C.J., Meyer, K.W., Carpenter, S.J., Erickson, J.M., Matsunaga, K.K.S., Smith, S.Y., Sheldon, N.D., 2016. Temperature and salinity of the Late Cretaceous Western Interior Seaway. Geology 44, 903–906. https://doi.org/10.1130/g38311.1.
Price, G.D., Page, K.N., 2008. A carbon and oxygen isotopic analysis of molluscan faunas from the Callovian–Oxfordian boundary at Redcliff Point, Weymouth, Dorset: implications for belemnite behaviour. Proc. Geol. Assoc. 119, 153–160. https://doi.org/10.1016/S0016-7878(08)80315-X.
Price, G.D., Passey, B.H., 2013. Dynamic polar climates in a greenhouse world: evidence from clumped isotope thermometry of Early Cretaceous belemnites. Geology 41, 923–926. https://doi.org/10.1130/g34484.1.
Price, G.D., Rogov, M.A., 2009. An isotopic appraisal of the Late Jurassic greenhouse phase in the Russian Platform. Palaeogeogr. Palaeoclimatol. Palaeoecol. 273, 41–49. https://doi.org/10.1016/j.palaeo.2008.11.011.
Price, G.D., Teece, C., 2010. Reconstructing of Jurassic (Bathonian) palaeosalinity using stable isotopes and faunal associations. J. Geol. Soc. Lond. 167, 1199–1208. https://doi.org/10.1144/0016-76492010-029.
Price, G.D., Hart, M.B., Wilby, P.R., Page, K.N., 2015. Isotopic analysis of Jurassic (Callovian) mollusks from the Christian Malford Laggerstätte (UK): implications for ocean water temperature estimates based on belemnoids. Palaios 30, 645–654. https://doi.org/10.1210/palo.2014.106.
Railsback, L.B., Anderson, T.F., Ackerly, S.C., Cisne, J.L., 1989. Paleoceanographic modeling of temperature-salinity profiles from stable isotopic data. Paleoceanography 4, 585–591. https://doi.org/10.1029/PA004i005p00585.
Riboulleau, A., Baudin, F., Daux, V., Hantzpergue, P., Renard, M., Zakharov, V., 1998. Évolution de la paléotemperature des eaux de la plate-forme russe au cours du Jurassique supérieur. C.R. Acad. Sci. IIA 326, 239–246.
Ritter, A.C., Movromatis, V., Dietzel, M., Kwiecien, O., Wiethoff, F., Griesshaber, E., Casella, L.A., Schmahl, W.W., Koelen, J., Neuser, R.D., Leis, A., Buhl, D., Niedermayr, A., Breitenbach, S.F.M., Bernasconi, S.M., Immenhauser, A., 2017. Exploring the impact of diagenesis on (isotope) geochemical and microstructural alteration features in biogenic aragonite. Sedimentology 64, 1354–1380. https://doi.org/10.1111/sed.12356.
Rogov, M.A., 2003. Upper Jurassic Ochetoceratinae (Oppeliidae, Ammonoidea) of Central Russia. Bull. Moscow Soc. Nat. 78, 38–52 (in Russian).
Rogov, M.A., 2017. Ammonites and infrazonal stratigraphy of the Kimmeridgian and Volgian stages of southern part of the Moscow Syneclise. Trans. Geol. Inst. 615, 7–160 (in Russian).
Rogov, M.A., Wierzbowski, A., Shchepetova, E., 2017. Ammonite assemblages in the Lower to Upper Kimmeridgian boundary interwal (Cymodoce to Mutabilis zones) of Tatarstan (central European Russia) and their correlation importance. N. Jb. Geol. Paläont. Abh. 285, 161–185. https://doi.org/10.1127/njgpa/2017/0675.
Rohling, E.J., 2013. Oxygen isotope composition of seawater. In: Elias, S.A. (Ed.), The Encyclopedia of Quaternary Science. Vol. 2. Elsevier, Amsterdam, pp. 915–922.
Rosales, I., Robles, S., Quesada, S., 2004. Elemental and oxygen isotope composition of Early Jurassic belemnites: salinity vs. temperature signals. J. Sediment. Res. 74, 342–354. https://doi.org/10.1306/112603740342.
Sælen, G., 1989. Diagenesis and construction of the belemnite rostrum. Palaeontology 32, 765–797.
Sahagian, D., Pinous, O., Olferiev, A., Zakharov, V., 1996. Eustatic curve for the Middle Jurassic–Cretaceous based on Russian Platform and Siberian stratigraphy: zonal resolution. AAPG Bull. 80, 1433–1458.
Savard, M.M., Veizer, J., Hinton, R., 1995. Cathodoluminescence at low Fe and Mn concentrations: a SIMS study of zones in natural calcites. J. Sediment. Res. A65, 208–213. https://doi.org/10.1306/d4268072-2b26-11d7-8648000102c1865d.
Sazonova, I.G., Sazonov, N.T., 1967. Paleogeografiya Russkoy Platformy v Yurskoe i Rannemelovoe Vremya. Ministerstvo Geologii SSSR. VNIGNI, Trudy, vypusk 62, Izdatelstvo, Nedra, Leningrad, pp. 253 In Russian.
Scherzinger, A., Schweigert, G., Fözy, I., 2016. First record of the Mediterranean zonal index *Mesosimoceras cavouri* (Gemmellaro, 1872) in the Upper Jurassic (Pseudomutabilis Zone, *semicostatum* γ horizon) of SW Germany and its stratigraphical significance. Vol. Jur. 14, 145–154. https://doi.org/10.5604/01.3001.0009.4020.
Shackleton, N.J., Kennett, J.P., 1975. Paleotemperature history of the Cenozoic and initiation of Antarctic glaciation: oxygen and carbon isotope analyses in DSDP sites 277, 279 and 281. Init. Rep. Deep Sea Drilling Proj. 29, 743–755. https://doi.org/10.2973/dsdp.proc.29.117.1975.
Shchepetova, E.V., Rogov, M.A., 2013. Organic carbon-rich horizons in the Upper Kimmeridgian of the northern part of Ulyanovsk-Saratov trough (Russian Platform): biostratigraphy, sedimentology, geochemistry. In: Zakharov, V.A., Rogov, M.A., Ippolitov, A.P. (Eds.), Jurassic System of Russia: Problems of Stratigraphy and Paleogeography, Fifth All Russian Meeting Makhachkala. Scientific Materials. ALEF, Makhachkala, pp. 249–252 September 15–20, 2015. (In Russian).
Shchepetova, E., Gavrilov, Y., Baraboshkin, E., Rogov, M., Shcherbinina, E., 2011. The main organic rich shale sequences in the Upper Jurassic and Lower Cretaceous of the Russian Platform: sedimentology, geochemistry and paleoenvironmental models. In: Matyja, B.A., Wierzbowski, A., Ziółkowski, P. (Eds.), Jurassica IX, Małogoszcz, 06-08 września 2011, Materiały Konferencyjne, Polskie Towarzystwo Geologiczne, Polska Grupa Robocza Systemu Jurajskiego, pp. 58–63.
Smelror, M., Mørk, A., Mørk, M.B.E., Weiss, H.M., Løseth, H., 2001. Middle Jurassic–Lower Cretaceous transgressive–regressive sequences and facies distribution off Northern Nordland and Troms, Norway. In: Martinsen, O.J., Dreyer, T. (Eds.), Sedimentary Environments Offshore Norway – Palaeozoic to Recent. Elsevier Science B.V, Amsterdam, pp. 211–232 NPF Special Publication 10.
Staudigel, P.T., Swart, P.K., 2016. Isotopic behavior during the aragonite-calcite transition: implications for sample preparation and proxy interpretation. Chem. Geol. 442, 130–138. https://doi.org/10.1016/j.chemgeo.2016.09.013.
Stevens, G.R., 1971. Relationship of isotopic temperatures and faunal realms to Jurassic-Cretaceous paleogeography, particularly of the South-West Pacific. J. Roy. Soc. New Zeal. 1, 145–158. https://doi.org/10.1080/03036758.1971.10419346.
Stevens, K., Griesshaber, E., Schmahl, W., Casella, L.A., Iba, Y., Mutterlose, J., 2017. Belemnite biomineralization, development, and geochemistry: the complex rostrum of *Neohibolites minimum*. Palaeogeogr. Palaeoclimatol. Palaeoecol. 468, 388–402. https://doi.org/10.1016/j.palaeo.2016.12.022.
Stolper, D.A., Eiler, J.M., 2015. The kinetics of solid-state isotope-exchange reactions for clumped isotopes: a study of inorganic calcites and apatites from natural and experimental samples. Am. J. Sci. 315, 363–411. https://doi.org/10.2475/05.2015.01.
Surge, D., Lohmann, K.C., 2008. Evaluating Mg/Ca ratios as a temperature proxy in the estuarine oyster, *Crassostrea virginica*. J. Geophys. Res. 113, G02001. https://doi.org/10.1029/2007jg000623.
Surge, D., Lohmann, K.C., Dettman, D.L., 2001. Controls on isotopic chemistry of the American oyster, *Crassostrea virginica*: implications for growth patterns. Palaeogeogr. Palaeoclimatol. Palaeoecol. 172, 283–296. https://doi.org/10.1016/s0031-0182(01)00303-0.
Surge, D.M., Lohmann, K.C., Goodfriend, G.A., 2003. Reconstructing estuarine conditions: oyster shells as recorders of environmental change, Southwest Florida. Estuar. Coast. Shelf S. 57, 737–756. https://doi.org/10.1016/s0272-7714(02)00370-0.
Swart, P.K., Price, R.M., Greer, L., 2001. Chapter 2: The relationship between stable isotopic variations (O, H, and C) and salinity in waters and corals from environments in South Florida: implications for reading the paleoenvironmental record. In: Wardlaw, B.R. (Ed.), Palaeoecological Studies of South Florida, pp. 17–29 Bulletins of American Paleontology 361.
Tesakova, E., 2008. Late Callovian and Early Oxfordian ostracods from the Dubki section (Saratov area, Russia): implications for stratigraphy, paleoecology, eustatic cycles and palaeobiogeography. Neues Jahrb. Geol. P.-A. 249, 25–45. https://doi.org/10.1127/0077-7749/2008/0249-0025.
Tesakova, E.M., 2014a. Jurassic Ostracods of the Russian Plate: stratigraphic Implications, Paleoecology and Paleogeography. D. Sci. Thesis. Moscow. pp. 455 in Russian.
Tesakova, E.M., 2014b. Palaeotemperature reconstruction of the Middle Russian Sea during the Middle and Late Jurassic by ostracods. In: Ivanov, A.V. (Ed.), Problems of Paleoecology and Historical Geoecology. Collection of Papers of All-Russian V.G. Ochev Scientific Conference. State Technical University of Saratov, Saratov, pp. 133–147 (in Russian).
Tesakova, E.M., 2017. Ostracods of the Virgatites virgatus zone from Moscow sections. In: Rogov, M.A., Mironenko, A.A., Guzhov, A.V., Tesakova, E.M., Ustinova, M.A., Shurupova, Y.A., Zverkov, N.G., Archangelsky, M.S., Shmakov, A.S., Baraboshkin, E.E. (Eds.), Jurassic Deposits if the Southern Part of the Moscow Synеclyse and their Fauna, pp. 301–310 Transactions of the Geological Institute 615. (In Russian).
Tesakova, E.M., Demidow, S.M., Guzhov, A.V., Rogov, M.A., Kiselev, D.N., 2012. Middle Oxfordian – Lower Kimmeridgian ostracod zones from the Mikhalenino section (Kostroma region) and their comparison with synchronous strata of the Eastern and Western Europe. Neues Jahrb. Geol. P.-A. 266, 239–249. https://doi.org/10.1127/0077-7749/2012/0281.
Thierry, J., Abbate, E., Alekseev, A.S., Ait-Ouali, R., Ait-Salem, H., Bouaziz, S., Canerot, J., Georgiev, G., Guiraud, R., Hirsch, F., Ivanik, M., Le Metour, J., Le Nindre, Y.M., Medina, F., Mouty, M., Nazarevich, B., Nikishin, A.M., Page, K., Panov, D.L., Pique, A., Poisson, A., Sandalescu, M., Sapunov, I.G., Seghedi, A., Soussi, M., Tchoumatchenko, P.V., Vaslet, D., Vishnevskaya, V., Volozh, V.A., Voznezenski, A., Walley, C.D., Wong, T.E., Ziegler, M., Barrier, E., Bergerat, F., Bracene, R., Brunet, M.F., Cadet, J.P., Guezou, J.C., Jabaloy, A., Lepvrier, C., Rimmele, G., De Wever, P., Baudin, F., Belaid, A., Bonneau, M., Coutelle, A., Fekirne, B., Guillocheau, F., Hantzpergue, M., Julien, M., Kokel, F., Lamarche, J., Mami, L., Mansy, J.L., Mascle, G., Pascal, C., Robin, C., Stephenson, R., Sihamdi, N., Vera, J.A., Vuks, V.J., 2000. Early Kimmeridgian. In: Dercourt, J., Gaetani, M., Vrielynck, B., Biju-Duval, B., Brunet, M.F., Cadet, J.P., Crasquin, S., Sandulescu, M. (Eds.), Atlas Peri-Tethys. Paleogeographical Maps, CCGM/CGMW, Paris, pp. 146–154 map 10.
Tobin, T.S., Wilson, G.P., Eiler, J.M., Hartmann, J.H., 2014. Environmental change across a terrestrial Cretaceous–Paleogene boundary section in eastern Montana, USA, constrained by carbonate clumped isotope paleothermometry. Geology 42, 351–354. https://doi.org/10.1130/G35262.1.
Tripati, A.K., Eagle, R.A., Thiagarajan, N., Gagnon, A.C., Bauch, H., Halloran, P.R., Eiler, J.M., 2010. ^{13}C–^{18}O isotope signatures and 'clumped isotope' thermometry in foraminifera and coccoliths. Geochim. Cosmochim. Acta 74, 5697–5717. https://doi.org/10.1016/j.gca.2010.07.006.
Tyson, R.V., Wilson, R.C.L., Downie, C., 1979. A stratified water column environmental model for the type Kimmeridge Clay. Nature 277, 377–380. https://doi.org/10.1038/

277377a0.
Ullmann, C.V., Korte, C., 2015. Diagenetic alteration in low-Mg calcite from macrofossils: a review. Geol. Q. 59, 3–20. https://doi.org/10.7306/gq.1217.
Ullmann, C.V., Pogge von Strandmann, P.A.E., 2017. The effect of shell secretion rate on Mg/Ca and Sr/Ca ratios in biogenic calcite as observed in a belemnite rostrum. Biogeosciences 14, 89–97. https://doi.org/10.5194/bg-14-89-2017.
Ullmann, C.V., Hesselbo, S.P., Korte, C., 2013. Tectonic forcing of Early to Middle Jurassic seawater Sr/Ca. Geology 41, 1211–1214. https://doi.org/10.1130/g34817.1.
Ullmann, C.V., Frei, R., Korte, C., Lüter, C., 2017. Element/Ca, C and O isotope ratios in modern brachiopods: species-specific signals of biomineralization. Chem. Geol. 460, 15–24. https://doi.org/10.1016/j.chemgeo.2017.03.034.
Ustinova, M.A., 2009. The distribution of calcareous nannofossils and foraminifers in the Callovian, Oxfordian, and Volgian deposits in the southwest of Moscow. Stratigr. Geol. Correl. 17, 204–217. https://doi.org/10.1134/S0869593809020087.
Ustinova, M.A., 2012. Foraminifers and stratigraphy of Middle Oxfordian – Lower Kimmeridgian of Kostroma Region (Mikhalenino section). Bull. Moscow Soc. Nat. 87, 43–52 (In Russian).
Ustinova, M.A., Tesakova, E.M., 2017. New data on microbiota of the Middle Volgian substage in the Loino section (Kirov Oblast). Stratigr. Geol. Correl. 25, 296–306.
Veizer, J., 1974. Chemical diagenesis of belemnite shells and possible consequences for paleotemperature determinations. Neues Jahrb. Geol. P-A. 147, 91–111.
Veizer, J., 1983. Chemical diagenesis of carbonates: theory and trace element technique. In: Arthur, M.A., Anderson, T.F., Kaplan, I.R., Veizer, J., Land, L.S. (Eds.), Stable Isotopes in Sedimentary Geology, pp. 3-1–3-100. SEPM Short Course No. 10, Dallas. https://doi.org/10.2110/scn.83.01.0000.
Wacker, U., Fiebig, J., Tödter, J., Schöne, B.R., Bahr, A., Friedrich, O., Tütken, T., Gischler, E., Joachimski, M.M., 2014. Empirical calibration of the clumped isotope paleothermometer using calcites of various origins. Geochim. Cosmochim. Acta 141, 127–144. https://doi.org/10.1016/j.gca.2014.06.004.
Wacker, U., Rutz, T., Löffler, N., Conrad, A.C., Tütken, T., Böttcher, M.E., Fiebig, J., 2016. Clumped isotope thermometry of carbonate-bearing apatite: revised sample pretreatment, acid digestion, and temperature calibration. Chem. Geol. 443, 97–110. https://doi.org/10.1016/j.chemgeo.2016.09.009.
Wanamaker, A.D., Kreutz, K.J., Wilson, T., Borns, H.W., Introne, D.S., Feindel, S., 2008. Experimentally determined Mg/Ca and Sr/Ca ratios in juvenile bivalve calcite for *Mytilus edulis*: implications for paleotemperature reconstructions. Geo-Mar. Lett. 28, 359–368. https://doi.org/10.1007/s00367-008-0112-8.
Westermann, G.E.G., 1996. Ammonoid Life and Habitat: Ammonoid Paleobiology. Plenum Press, New-York, pp. 607–707.
Wierzbowski, H., 2015. Seawater temperatures and carbon isotope variations in central European basins at the Middle–Late Jurassic transition (Late Callovian–Early Kimmeridgian). Palaeogeogr. Palaeoclimatol. Palaeoecol. 440, 506–523. https://doi.org/10.1016/j.palaeo.2015.09.020.
Wierzbowski, H., Joachimski, M., 2007. Reconstruction of late Bajocian–Bathonian marine palaeoenvironments using carbon and oxygen isotope ratios of calcareous fossils from the Polish Jura Chain (Central Poland). Palaeogeogr. Palaeoclimatol. Palaeoecol. 254, 523–540. https://doi.org/10.1016/j.palaeo.2007.07.010.
Wierzbowski, H., Joachimski, M.M., 2009. Stable isotopes, elemental distribution, and growth rings of belemnopsid belemnite rostra: proxies for belemnite life habitat. Palaios 24, 377–386. https://doi.org/10.2110/palo.2008.p08-101r.
Wierzbowski, A., Matyja, B.A., 2014. Ammonite biostratigraphy in the Polish Jura sections (Central Poland) as a clue for recognition of the uniform base of the Kimmeridgian Stage. Vol. Jur. 12, 45–98.
Wierzbowski, H., Rogov, M.A., 2011. Reconstructing the palaeoenvironment of the Middle Russian Sea during the Middle–Late Jurassic transition using stable isotope ratios of cephalopod shells and variations in faunal assemblages. Palaeogeogr. Palaeoclimatol. Palaeoecol. 299, 250–264. https://doi.org/10.1016/j.palaeo.2010.11.006.
Wierzbowski, H., Dembicz, K., Praszkier, T., 2009. Oxygen and carbon isotope composition of Callovian–Lower Oxfordian (Middle–Upper Jurassic) belemnite rostra from Central Poland: a record of a Late Callovian global sea-level rise? Palaeogeogr. Palaeoclimatol. Palaeoecol. 283, 182–194. https://doi.org/10.1016/j.palaeo.2009.09.020.
Wierzbowski, H., Rogov, M.A., Matyja, B.A., Kiselev, D., Ippolitov, A., 2013. Middle–Upper Jurassic (Upper Callovian–Lower Kimmeridgian) stable isotope and elemental records of the Russian Platform: indices of oceanographic and climatic changes. Glob. Planet. Chang. 107, 196–212. https://doi.org/10.1016/j.gloplacha.2013.05.011.
Wierzbowski, A., Smoleń, J., Iwańczuk, J., 2015. The Oxfordian and Lower Kimmeridgian of the Peri-Baltic Syneclise (North-Eastern Poland): stratigraphy, ammonites, microfossils (foraminifers, radiolarians), facies, and palaeogeographical implications. Neues Jahrb. Geol. P-A. 277, 63–104. https://doi.org/10.1127/njgpa/2015/0496.
Wierzbowski, H., Anczkiewicz, R., Pawlak, J., Rogov, M.A., Kuznetsov, A.B., 2017. Revised Middle–Upper Jurassic strontium isotope stratigraphy. Chem. Geol. 466, 239–255. https://doi.org/10.1016/j.chemgeo.2017.05.015.
Wignall, P.B., Hallam, A., 1991. Biofacies, stratigraphic distribution and depositional models of British onshore Jurassic black shales. In: Tyson, R.V., Pearson, T.H. (Eds.), Modern and Ancient Continental Shelf Anoxia, pp. 291–309. Geological Society Special Publication No 58. https://doi.org/10.1144/GSL.SP.1991.058.01.19.
Yasuhara, M., Okahashi, H., Cronin, T.M., 2009. Taxonomy of Quaternary deep-sea ostracods from the Western North Atlantic Ocean. Palaeontology 52, 879–931. https://doi.org/10.1111/j.1475-4983.2009.00888.x.
Yoshioka, S., Kitano, Y., 1985. Transformation of aragonite to calcite through heating. Geochem. J. 19, 245–249. https://doi.org/10.2343/geochemj.19.245.
Žak, K., Košťak, M., Man, o., Zakharov, V.A., Rogov, M.A., Pruner, P., Rohovec, J., Dzuba, O.S., Mazuch, M., 2011. Comparison of carbonate C and O stable isotope records across the Jurassic/Cretaceous boundary in the Tethyan and Boreal Realms. Palaeogeogr. Palaeoclimatol. Palaeoecol. 299, 83–96. https://doi.org/10.1016/j.palaeo.2010.10.038.
Zakharov, V.A., Rogov, M.A., 2003. Boreal-Tethyan mollusk migrations at the Jurassic–Cretaceous boundary time and biogeographic ecotone position in the Northern Hemisphere. Stratigr. Geol. Corr. 11, 152–171.
Zakharov, V.A., Rogov, M.A., Shchepetova, E.V., 2017. Black shale events in the Late Jurassic–earliest Cretaceous of Central Russia. In: Zakharov, V.A., Rogov, M.A., Shchepetova, E.V. (Eds.), Jurassic System of Russia: Problems of Stratigraphy and Paleogeography. Seventh all-Russian Conference. Scientific Materials, Moscow, pp. 57–63 In Russian.
Zhou, J., Poulsen, C.J., Pollard, D., White, T.S., 2008. Simulation of modern and middle Cretaceous marine $\delta^{18}O$ with and ocean-atmosphere general circulation model. Paleoceanography 23, PA3223. https://doi.org/10.1029/2008PA001596.2008.
Zuev, G.V., Nesis, K.N., 1971. Kal'mary (Biologiya i Promysel). Pishchevaya Promyshlennost, Moskva, pp. 360 In Russian.